Ocean Engineering 250 (2022) 110572

Contents lists available at ScienceDirect

Ocean Engineering

journal homepage: www.elsevier.com/locate/oceaneng

Numerical investigation on mooring line configurations of a Paired Column Semisubmersible for its global performance in deep water condition

Chiemela Victor Amaechi [a,d,*], Agbomerie Charles Odijie [b], Facheng Wang [c], Jianqiao Ye [a,**]

[a] Department of Engineering, Lancaster University, Lancaster, LA1 4YR, UK
[b] Department of Engineering, MSCM Limited, High Wycombe, Oxfordshire, HP12 3TA, UK
[c] Department of Civil Engineering, Tsinghua University, Beijing, 100084, China
[d] Standards Organisation of Nigeria (SON), 52 Lome Crescent, Wuse Zone 7, Abuja, Nigeria

ARTICLE INFO

Keywords:
Paired column semisubmersible (PCSemi)
Catenary mooring system
Hydrodynamics
Mooring lines
Offshore platform
Semisubmersible global performance

ABSTRACT

The advances observed in the offshore-renewable industry include the recent development of a deep draft paired column semisubmersible platform developed for application on dry trees in Gulf of Mexico (GoM). These developments led to the recent innovation of the Paired Column Semisubmersible by Jun Zou of Houston Offshore Engineering. This paper presents a detailed investigation on the mooring line analysis for two different configurations on the hull of a Paired Column Semisubmersible (PCSemi). The numerical research of the PCSemi platform coupled with mooring lines was conducted, and the model was validated. Two different mooring configurations were investigated: Chain-Polyester-Chain (CPC) and Polyester-Polyester (PP) configurations, with dynamic coupling in frequency domain (FD) and time domain (TD) using ANSYS AQWA and Orcaflex. A comparative study of the mooring lines is also investigated in 2,438 m water depth at GoM, using 16 mooring lines with catenary mooring design. Results of this study gives the natural period of floating PCSemi's heave motion ranged from 21s to 22s. Also, the effect of a damaged mooring line increased the tension in other mooring lines. Lastly, the CPC configuration has a smaller amplitude for wave-frequency platform motions compared to the PP mooring configuration from the depicted PCSemi global performance.

1. Introduction

The increasing demand for oil and gas supply has also increased despite the increase in the application of renewable resources globally in the offshore-renewable industry. This demand has also led to the increased exploration of oil and gas products within the offshore sector. It has also led to crude oil explorations tending towards more challenging, more profound, and complicated locations to explore. These locations include the remote areas of Western Australian Offshore Areas (WAOA), Offshore Brazil Pre-Salt (BPS), North Sea (NS), China Sea (CS), Persian Sea (PS), Offshore West Africa (OWA) like Bonny in the Niger Delta location of Nigeria, and other ultra-deepwater reservoirs in the Gulf of Mexico (GoM). These areas require heavy machinery for drilling or production, such as offshore floating platforms with high characteristic strength and better motion performance. This will help it to withstand both environmental and operational challenges (Amaechi et al., 2022a, 2022b). Secondly, due to the uncertainty of challenging environmental conditions, oil wells, and oil reservoirs, the application of large drilling rigs with variable payloads may be needed. This points to the fact that the structures would need stability. Stability can be achieved by restraining the floating offshore structures (F.O.S) and anchoring them. Thus, moored cables called mooring lines are generally used to hold it in position. Thirdly, floating structures like PCSemi have very large topsides that require more extensive space, have large sizes and great weight (Odijie, 2016; Zou, 2014). Thus, additional loads from moorings imply that mooring lines also challenge these massive floating structures (Ja'e et al., 2022; Ali et al., 2020). In addition to the moorings, there are other attachments like marine risers and hoses that add to the loadings of the floating structure (Amaechi et al., 2022c, 2022d, 2022e).

Different researchers have investigated mooring lines on various floating forms like PCSemis (Das and Zou, 2015; Zou J. 2014; Bhosale D. 2017; Odijie et al., 2017), semisubmersible-type VLFS (Wang Y. et al., 2018; Wang C.M et al., 2008), drillship FPSOs (Ma G., Sun L. & Wang H., 2009; Mazaheri S. & Mesbahi E., 2003; Mazaheri S. & Incesik A., 2004),

* Corresponding author. Department of Engineering, Lancaster University, Lancaster, LA1 4YR, UK
** Corresponding author.
E-mail addresses: c.amaechi@lancaster.ac.uk (C.V. Amaechi), j.ye2@lancaster.ac.uk (J. Ye).

https://doi.org/10.1016/j.oceaneng.2022.110572
Received 8 May 2021; Received in revised form 12 December 2021; Accepted 5 January 2022
Available online 14 March 2022

Abbreviations list

6DoF	Six Degrees of Freedom
A	Area of body
A/D	Area/Depth ratio
ABS	American Bureau of Shipping
API	American Petroleum Institute
BEM	Boundary Element Method
BPS	Brazil Pre-Salt
BS	British Standard
C_a	Added Mass Coefficient
CAPEX	Capital Expenditure
C_d	Drag Coefficient
CFD	Computational Fluid Dynamics
CoG	Centre of Gravity
CPC	Chain Polyester Chain
CPR	Composite Production Riser
CS	China Sea
DDSemi	Deep Draft Semisubmersible
DIC	Digital Image Capture
DNVGL	Det Norske Veritas & Germanischer Lloyd
D.P	Dynamic positioning
FD	Frequency Domain
FEA	Finite Element Analysis
FEM	Finite Element Model
FOS	Floating Offshore Structure
FPSO	Floating Production, Storage and Offloading
FRF	Fixed Reference Frame
FSI	Fluid-Structure Interaction
GoM	Gulf of Mexico
GRF	Global Reference Frame
HOE	Houston Offshore Engineering
INT	Interim
ISO	International Standardisation Organisation
JONSWAP	Joint North Sea Wave Project
MBL	Maximum Breaking Load
MET	Metocean
MFA	Mega-Floating Airport
ML13	Mooring Line 13
ML14	Mooring Line 14
ML15	Mooring Line 15
ML16	Mooring Line 16
NS	North Sea
OCIMF	Oil Companies International Marine Forum
OWA	Offshore West Africa
PCSemi	Paired Column Semisubmersible
PP	Polyester-Polyester
PS	Persian Sea
R4	Grade R4 Studless Chain
RAO	Response Amplitude Operator
RPSEA	Research Partnership to Secure Energy for America
SCR	Steel Catenary Riser
SON	Standards Organisation of Nigeria
SPAR	Single Point Anchor Reservoir
TD	Time Domain
TDP	Touch Down Point
TLP	Tension Leg Platform
TTR	Top Tensioned Riser
USA	United States of America
V	Volume of body
V_r	Relative velocity of fluid particles
VIM	Vortex-Induced Motion
VIV	Vortex-Induced Vibration
VLFS	Very Large Floating Structures
WAOA	Western Australian Offshore Areas
WEC	Wave Energy Converter

genetic algorithm optimization (Rezvani A. & Shafieefar M., 2007; Alonso J.J.C. et al., 2005; Maffra S., Pacheo C. & Menezez M., 2003, Mirzaei et al., 2014), floating bridges (Daghigh M., Paein Loulaei R.T. & Seif M.S., 2002), coupling analysis (Bhosale D. 2017; Garrett D.L., 2005, 1982), as well as general floating structures (Barltrop, N. D. P., 2003; Brebbia, 1979; Newman, 1999; Wilson J.F. 2008). Also, different loadings influence the dynamics of moorings. These include snap tension (Su-xia Z. et al., 2009), fatigue life (Das and Zou, 2015; Lassen T. et al., 2009), current loads (Odijie C. 2016; Stansberg C.T., 2008), mooring stiffness (Bhosale D. 2017; Huilong R., Jian Z., Guoqing F., Hui L. & Chenfeng L., 2009), low-frequency motion (Waals O.J., 2009; Hadi Sabziyan et al., 2014; Wu, S., 1997), and dynamic operation (Jordan M. A., Beltran-Aguedo R. 2004; Chen, X. H., 1997; Morch, M., and Moan, T., 1985). A descriptive schematic of a taut mooring and a catenary mooring system is depicted in Fig. 1.

In recent times, FOS like the semisubmersible, SPAR (Single Point Anchor Reservoir) and TLP (Tension Leg Platform) have increased application in deep water, but Zou et al. (2014) reported that only the SPARS and TLPs were the only two proven dry tree hull forms in deep water field development which led to the development of the Paired Column Semisubmersible (PCSemi) Platform, by Jun Zou and his design team at Houston Offshore Engineering (HOE), now an Atkins Company, U.S.A. first reported in Zou (2008), and concept developed further (RPSEA, 2009; Zou et al., 2013, 2014; Das and Zou, 2015). However, it is noteworthy that the TLP becomes highly expensive and sometimes with prohibitive cost implications in deep water increase beyond 1,646 m, leaving the SPAR as the only dry-tree hull form that has proved highly effective in such depths beyond 1,646 m (Zou et al. 2014). With large dry-tree platforms come a large drilling rig with large deck space. This space is used for the drilling stack storage and the entire drilling operation workspace. Although, the challenge with SPARS is that the large space becomes an issue with offshore installation, dry transport, and mobilization to the new reservoir. However, considering that semisubmersibles have a hull form designed to provide large deck space, large storage space, and quayside integration over SPARS, as such becomes better in terms of the economy over the SPAR platform has larger topsides payloads. Thus, the need for a more sustainable and all-encompassing dry tree solution can reduce the field development costs in terms of CAPEX (capital expenditure) savings (Zou J. et al., 2017). These considerations are in terms of the designing, analysis, engineering, fabrication, prototyping, testing, installation, pre-commissioning of the hull, mooring, risers, topsides and other component development (Bai and Bai, 2005; Kim C.H. 2008; Brebbia C. A. 1979; Sarpkaya T.S. 2010; Wilson J.F. 2008). Aside from semisubmersibles, other FOS developments like Very Large Floating Structures (VLFS) have increased. These include the large-scale floating airport in China, Mega-Floating Airport (MFA) such as proposed in the challenging development of the test runway in the floating terminal of Kansai International Airport Japan (Wang Y. et al., 2018; Okamura H. 2000), the floating football stadium in Angola constructed in 2019, the floating football stadium in Kho Panyee Thailand restored in 2018, Achmad Yani International Airport which is the first floating airport in the world completed in 2018 with a floating terminal (Andrianov, A.O.I. 2005; Ohmatsu S. 2005; Suzuki H. 2005; Taguchi Aki and Tomoi Takehito, 2001). However, these so-called mega-floats structures are classical pontoon-type VLFS, but they are challenged by hydroelastic responses, buoyancy and motion responses (Wang C.M et al., 2008; Bishop and Price, 2005; Bai and Bai, 2005). Thus, the need to be

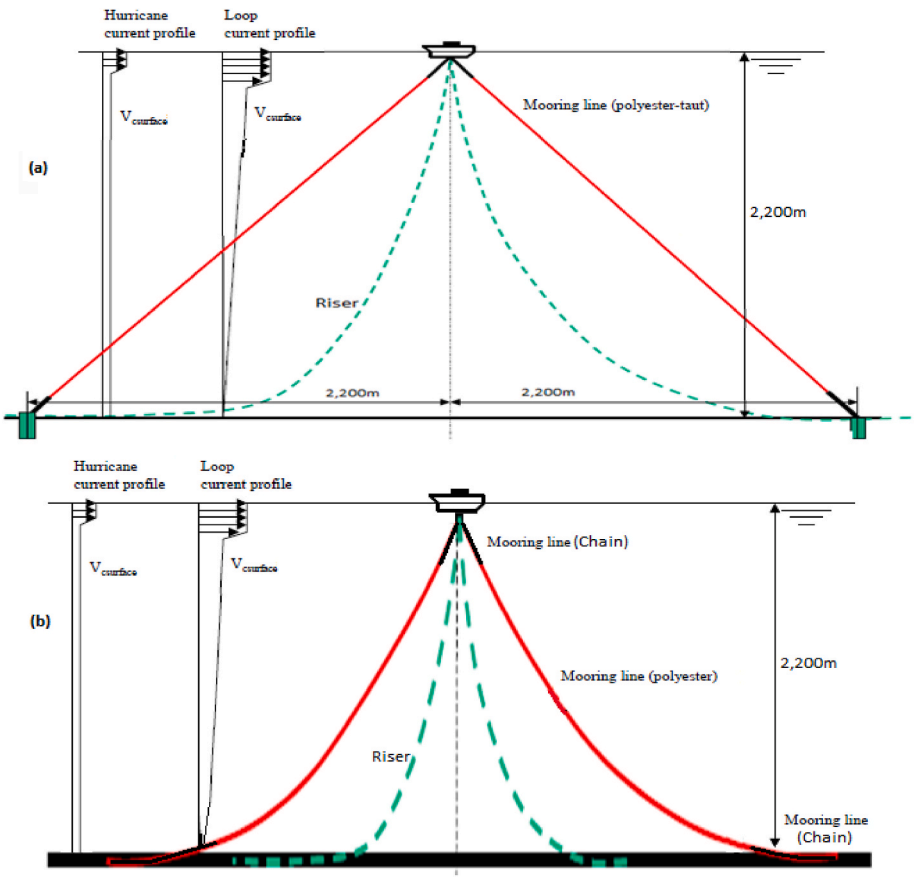

Fig. 1. Schematic of Mooring lines, showing (a) Taut Mooring Lines, and (b) Catenary Mooring lines.

properly restrained with cables, tendons and mooring lines. This challenge is influenced by the large length-to-thickness ratio structure, similar to that of attached marine risers and marine hoses (Amaechi et al., 2019a, 2019b; 2019c; 2019d; 2021a; 2021b; 2021c; Amaechi and Ye, 2021). Nevertheless, the advantage of PCSemi over the deep-draft and traditional semisubmersible has led to recent advances in PCSemi (Odijie and Ye, 2015; Odijie et al. 2015, 2017; Odijie, 2016). Odijie and Ye (2015b) presented an understanding of fluid-structure interaction (FSI) for high amplitude wave loadings on PC Semi. The authors applied a finite element approach using ANSYS AQWA and Orcaflex, as detailed in Odijie (2016). The study presented was on the global performance of PCSemi, with motion characteristics for RAOs, added masses, first order forces and second-order forces and the effect of environmental conditions, currents and draft sizes of the PCSemi but presented very scanty discussion on the mooring analysis. However, this investigation was further developed as presented in another study (Bhosale D. 2017), by using ANSYS AQWA to numerically conduct the mooring analysis for the PCSemi. The study considered three cases of moorings but concluded that the results were subject to further investigation based on integrity of the moorings and some experimental tests. In another study, Das and Zou (2015) presented a detailed investigation on the global performance and included some details on the marine risers and mooring lines, but did not include any detail on the mooring analysis. Odijie and Ye (2015b) investigated on the effect of vortex induced vibration on a PCSemi but did not include the effect of moorings on the study. However, this was covered in another study by Zou J. (2014). In this study, the vortex-induced motion (VIM) response of the PCSemi was investigated with its effects on mooring fatigue, by using two sets of A/D envelope curves and three defined cases of two different PCSemis and one DDSemi, with other motion studies (Zou J. 2008; 2017a; 2017b; Zou J. et al., 2011, 2012). The conclusion was that increasing the chain sizes of the mooring lines increased the mooring fatigue. However, the study did not consider the stiffness effects of polyester moorings on the mooring fatigue, and mooring pretension effects on the mooring fatigue, but the study also proved that the PCSemi had superior VIM responses as predicted in the concept study (Zou J. 2017) and that it is a host platform that is mooring-fatigue-friendly (Zou J. 2014).

In this study, a numerical investigation on the global performance with mooring analysis is conducted on a paired column semisubmersible platform. This study presents a detailed research on mooring dynamics, mooring tensions, and the global performance of PCSemi under different mooring cases in deep water conditions. The mooring analysis was performed using a dynamic coupled approach and the numerical tools utilised are ANSYS AQWA and Orcaflex. Some comparative studies were carried out on this hydrodynamic investigation to evaluate the behaviour of similar and dissimilar mooring lines. In addition, some operational conditions were considered, like the intact and damaged conditions. In this study, the theory and governing equations are presented in Section 2. The numerical model, including the model description, the mesh study, and the component design, are presented in Section 3. The materials, methodology, environmental conditions, and model validation for the mooring analysis are presented in Section 4, while the result analysis and discussion are presented in Section 5. The conclusions and recommendations made on this numerical investigation are presented in Section 6.

2. Numerical model

2.1. Model description

In the numerical modelling, there were two different numerical models developed and utilised in this investigation. They are the finite

element model (FEM) and a hydrodynamic model based on Boundary Element Method (BEM). The BEM theory, which was formulated using potential flow theory (Amaechi et al., 2019a, 2021d, 2021e, 2021f). This theory was applied to develop the hydrodynamic model in ANSYS AQWA (ANSYS, 2017a; 2017b). The motion responses and force parameters for this PC Semi hull were calculated using this model (Odijie, 2016; Odijie and Ye, 2015). However, a good understanding of the diffracted and radiation wave conditions is required to describe the dynamic effect of the fluid-structure interactions on the strength and stability of the columns for large floating bodies such as a PCSemi hull. Based on the wave propagation on the PCSemi illustrated in Fig. 2, the wave elevation creates an angle on the XY plan, known as the 'wave direction'. Details on the technique used for estimating the second order drift forces considering the two groups of regular waves travelling at different phase angles, amplitudes, directions and frequencies exist in literature (Brorsen, 2006; Langley, 1984; Yamaguchi et al., 2005; Newman, 1974).

The main structure applied in this investigation is the PCSemi. The marine riser integration and the mooring analysis were carried out, as both the risers and mooring lines are dependent structures. The PCSemi is a floating offshore structure (FOS) is made up of four inner columns and four outer columns. This is illustrated with the components labelled in Figs. 3 and 4, while the dimensions for the PCSemi hull are presented in Fig. 5 and Table 1. In principle, the design, as considered by Zou (2014) and Odijie C. (2016), was that the geometrical configuration of the outer columns are square whereas the inner columns are rectangular, and that is maintained in this present study. The inside columns are designed as load-bearing columns to bear the topside load, whereas the outer columns support the structure with the provision of the stability and buoyancy required. The PCSemi was designed to be operated in deep waters and ultra-deep waters; thus, the PCSemi is a deep draft, implying that it is pretty stable but also susceptible to extreme wave and current loadings (RPSEA, 2009; Odijie C. 2016; Bhosale D. 2017).

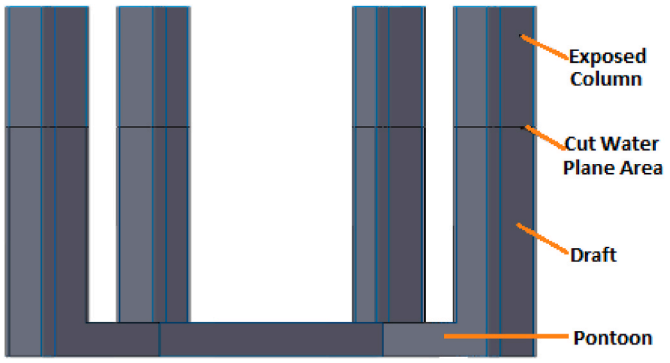

Fig. 3. Component parts of the paired column semisubmersible hull.

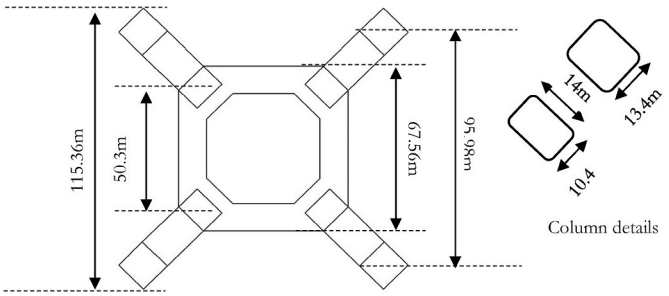

Fig. 4. Details of the dimensions for the Paired Column Semisubmersible Hull.

2.2. Finite element model (FEM)

The finite element model for the PCSemi is shown in Figs. 5 and 6. It was designed in Solidworks 2020 and then imported into ANSYS AQWA R2 2020 (ANSYS, 2017a; 2017b; 2017c) and Orcaflex 11.0f (Orcina,

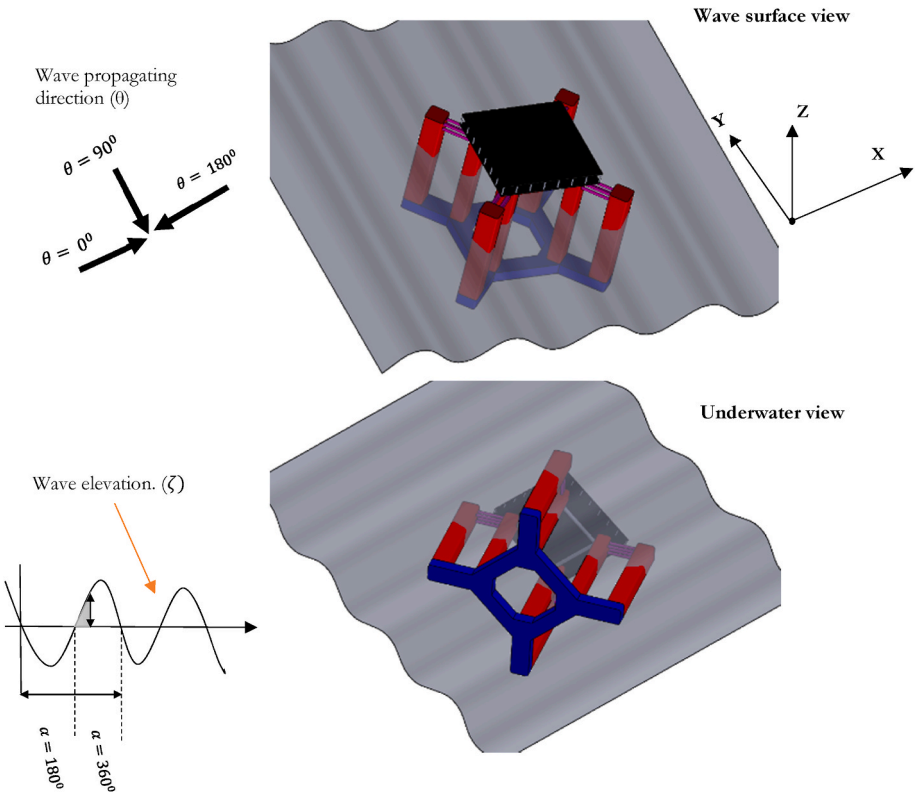

Fig. 2. Wave definition on PC Semi (Courtesy: Odijie, 2016).

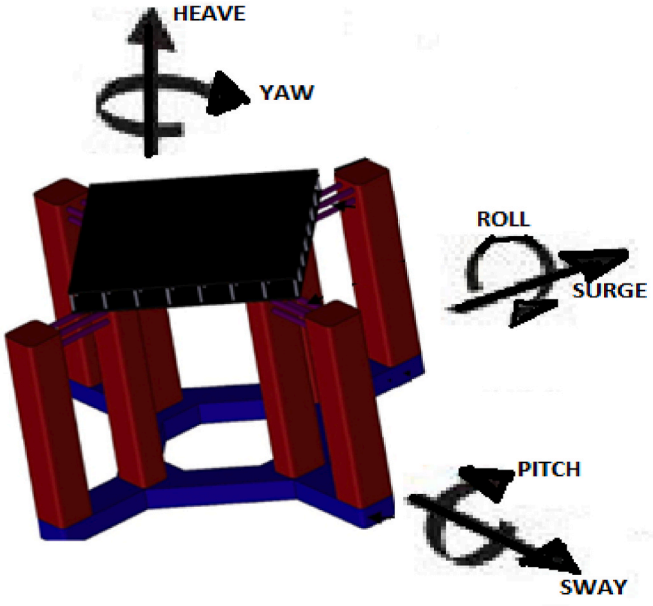

Fig. 5. The 6 DoF motions for the Paired Column Semisubmersible.

Table 1
Parameters of the PC semi hull.

Particulars	Values	Unit
Water depth	2438.4	m
Draft	53.34	m
Displacement	98,743,000	kg
Inner Column	4	–
Outer Column	4	–
Inner Column Dimension	10.4 × 14	m
Outer Column Dimension	13.4 × 14	m
Inner Column Span	50.3	m
Outer Column Span	95.98	m
Pontoon Height	7.92	m
Fairlead Level	49	m

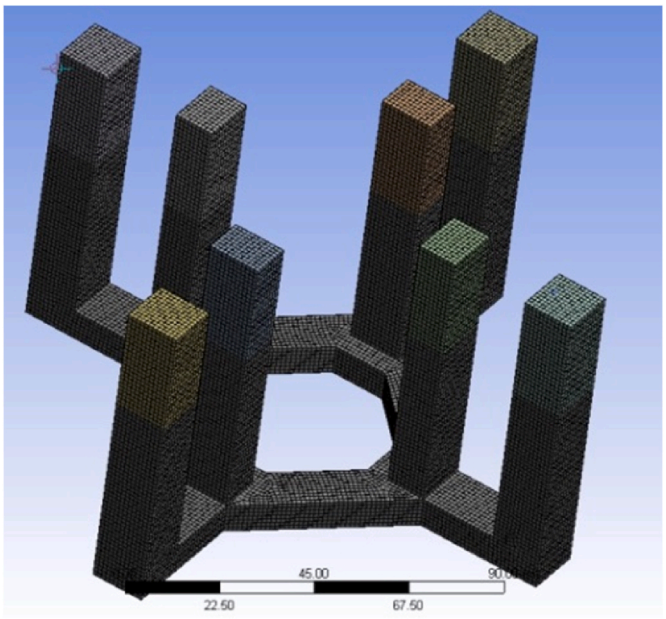

Fig. 6. PC Semi model without topside (in ANSYS R2 2020).

2014, 2021) as a Parasolid file. Two different configurations were considered in the mooring design, as discussed in subsequent sections. The deep water ocean condition was considered, but no effect of marine growth was assessed on the mooring lines or marine risers. The 6DoFs for the floating PCSemi are illustrated in Fig. 5.

2.3. Hydrodynamic model

The model was developed in ANSYS AWQA using the prescribed model in Section 2.1. The full-scale model dimension was extracted from RPSEA report (RPSEA, 2009) with slight alteration for the column height and edges, to help increase result accuracy. ANSYS AWQA utilised diffraction/radiation methods to resolve the three-dimensional (3D) problem of floating bodies. This method is generally acceptable in ocean engineering, as it eliminates the complexity associated with the water viscosity, flow separation, and circulation. Different research works and extensive reports have been documented and published based on applying this technique to resolve the behaviour of large floating bodies. This technique has been validated in free-floating conditions considered and existent in similar studies on hydrodynamic loading on PCSemi (RPSEA, 2009; Odijie et al., 2017; Odijie C.A. 2016; Bhosale D. 2017; Zou J. 2014, 2017; Das S. et al., 2015). Aside from this, offshore engineers could employ experimental and analytical methods, but these methods are restricted. The hydrodynamic panel model for the PCSemi is shown in Fig. 7. The hydrodynamic diffraction analysis was developed in ANSYS AQWA R2 2020 for specific sea and weather conditions. The hull model for this analysis was selected from the already designed PCSemis, as seen in Table 1. During the free-floating conditions, the effect of topside, moorings, risers, and other structural attachments were not considered. The impact pressure results at different flow directions were recorded. The pressure and motion results resolved from the diffraction analysis were used as ocean loadings for the finite element analysis. Emphasis was placed on investigating the hydrodynamic pressure forces acting on each element and node for various flow orientations using a time series analysis. The global design conducted in this investigation was carried out under irregular waves, and the damping was calculated by applying the Morison Equation (Morison et al., 1950). The modified Morison's equation is expressed in Equation

Fig. 7. Hydrodynamic panel model of the PC semi (in ANSYS AQWA R2 2020).

(1), where V is the volume of the body, $\mathbf{V_r}$ is the relative velocity of fluid particles, A is the area of the body, C_d is the drag coefficient, C_a is the added mass coefficient.

$$\boldsymbol{F} = (\Delta \boldsymbol{a}_w + \boldsymbol{\rho C}_a \Delta \boldsymbol{a}_r) + \frac{1}{2}\boldsymbol{\rho C}_d \boldsymbol{A V}_r |\boldsymbol{V}_r| \quad (1)$$

2.4. Mesh study

Mesh independence study was carried out on the hull model designed for hydrodynamic analysis to help increase the accuracy of the result. For the effectiveness of mess density and tolerance, the element size was varied between 2 m and 1.15 m. The effects on the maximum RAO at 0° incidences in the Z direction were recorded. An illustration of this effect is visible in the panel models with element sizes for 5 m and 2 m, shown in Fig. 8. From this mesh study, the maximum heave RAO is represented in Table 2. The results in Table 2 show no significant variation in the RAO value for heave motion at 0° flow angle for the same range of wave frequencies. This indicates that the degree of mesh refinement does not significantly affect results from hydrodynamic diffraction study. It is pertinent to mention that only basic meshing was performed without further mesh refinement on any particular hull section. The hydrodynamic mesh considered is the element size 1.15 m, applied to obtain the panel model in Fig. 7. Straight edges were considered for mesh uniformity along the hull, as the hydrodynamic panel was without any mooring cable. Fig. 9 shows the element's graphical representation, including the details of the chosen element size of 1.15 m.

2.5. Component design

The component design was based on the hydrodynamic model. The depth of the seabed in the model is also based on the structure's actual operating depth, which is 2438.4 m. The hydrodynamic domain area for this analysis is kept as 7000 m × 7000 m, as shown in Fig. 10. The Hydrostatic properties of the geometry are presented in Section 4.4. In ANSYS AQWA R2 2020, the Global Reference Frame (GRF) and a Fixed Reference Frame (FRF) were applied, as shown in the hydrodynamic domain in Fig. 11. The Fixed Reference Frame lies on the structure geometry at the cut water plane area. Any displacement in the position of the structure causes a displacement of the Fixed Reference Frame. In the same vein, this Fixed Reference has axes that lie parallel to the Global Reference Frame. The relative position of the structure to the Global Reference Frame is not a significant concern since most of the forces are applied relative to the Fixed Reference Frame. The Centre of Mass of the structure is also given relative to the Fixed Reference Frame. For clarity, the positive axes of the fixed reference frame are defined as follows: X-axis, Y-axis, and Z-axis. The **X-Axis** lies parallel to the global X-axis. The positive direction of the X-axis is also the direction of wave propagation. It lies on the water plane area, while its origin is positioned in the centre of the geometry. The second is that the Y-Axis is perpendicular to wave propagation and lies in the horizontal plane on the water plane area. This plane also has the origin placed at the centre of the geometry. The third is the **Z-Axis,** which is the positive, usually upwards, perpendicular to the horizontal plane. It points upwards from the free surface, while its origin is also located on the cut water plane area.

Table 2
Mesh study using the Heave RAO for the PC Semi hull.

Element size (m)	No. of nodes	No. of elements	Max. RAO (m/m)
1.15	25536	25140	1.711
1.2	24237	24055	1.731
1.4	18215	18061	1.736
1.6	14061	13925	1.740
1.8	11374	11252	1.738
2.0	9058	8948	1.747

2.6. Mooring lines

The design of the mooring line was developed using the schematic concept of the different components that make up a mooring line, as illustrated in Fig. 1. Thus, the numerical model had to consider different factors in the selection of the materials for the mooring lines. This includes the material weight, stiffness, manufacturing, duration of tethering, size of floating offshore structure, the location, the water depth, and the space allocation. Of all these factors, the density (weight) and the space allocation for the mooring lines is highly pertinent during the design stage as it can affect the selection of the mooring configuration, as in Figs. 10 and 12. The mooring analysis being performed in this study is a Dynamic Coupled Analysis. Both the structure and the mooring lines were analysed together as a system. ANSYS AQWA R2 2020 and Orcaflex 11.0f were used in this numerical study. These numerical simulation tools have been validated and used to model floating and fixed offshore structures (Amaechi et al., 2019a; Odijie et al., 2017; Odijie and Ye, 2015). The analysis is performed by subjecting these models to external forces and measuring their responses as a result.

The structure of interest in this mooring analysis is the PCSemi. An analysis of the 16 mooring lines and 12 mooring lines was carried out, as shown in Fig. 12. This design is relatively recent and is currently undergoing further research. The structure is made up of four inner columns and four outer columns. Generally, the outer columns are square whereas the inner columns are rectangular in configuration. The inside columns are designed to bear the topside load while the outer columns provide the structure much-needed stability and buoyancy. The PCSemi was designed to be operated in ultra-deep waters. Details of the two configurations for the mooring lines are presented in Figs. 12 and 13. The structure also has a deep draft meaning it is quite stable and susceptible to extreme wave and current loadings. The details on the fixed points, connection points, mooring azimuths and pretensions are given

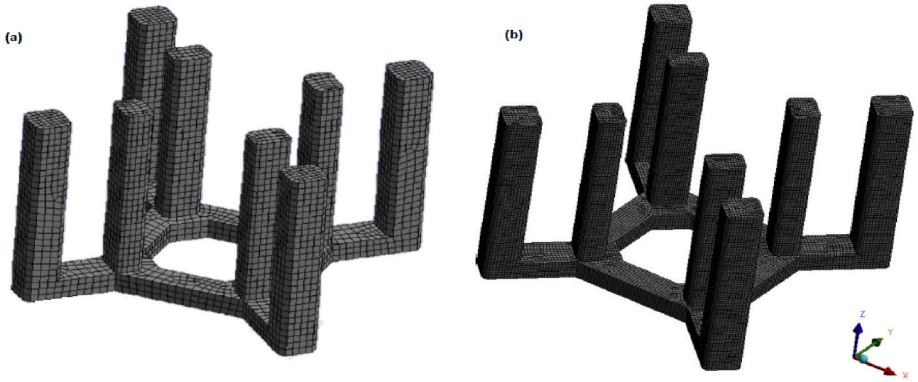

Fig. 8. Mesh study for panel models with element sizes (a) 5 m and (b) 2 m (in ANSYS AQWA R2 2020).

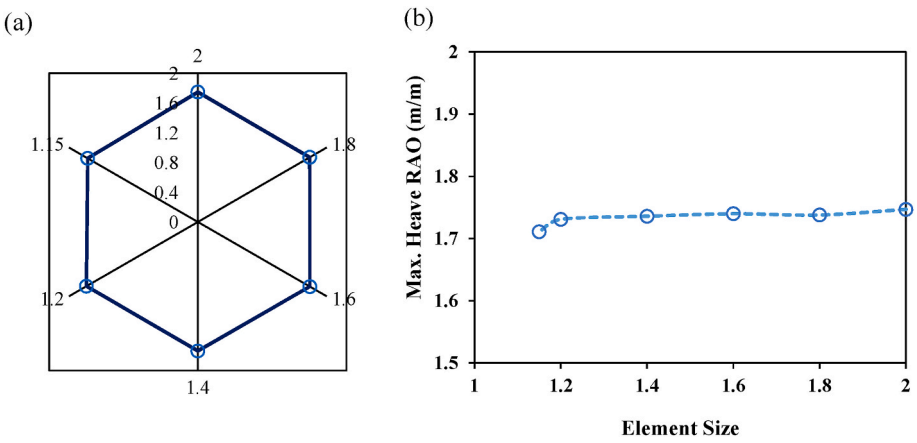

Fig. 9. Mesh Study for the panel model showing (a) radar plot, and (b) line plot.

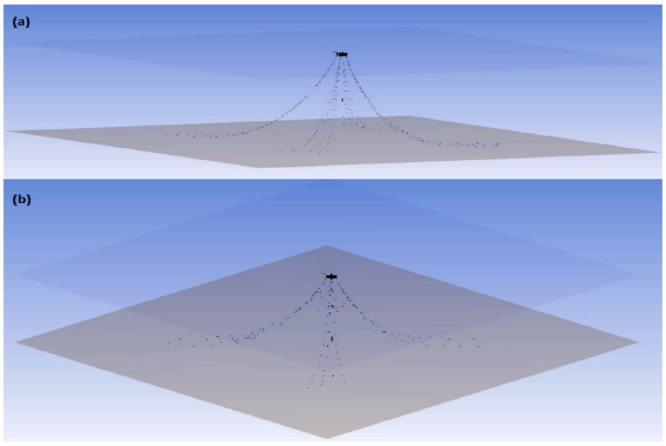

Fig. 10. Hydrodynamic domain showing PC Semi with catenary mooring lines in ANSYS AQWA.

in Tables 3–5. Due to the unbalanced loads emanating from the risers, particularly the SCRs (including water injection, production risers and the umbilicals), there is an asymmetric arrangement on the pretension for the mooring system. This mooring constitution is based on similar existing platform in the GoM called the Mad Dog SPAR platform, and another study by Zou et al. (2014a,b). Table 5 was obtained from PCSemi study by Das and Zou (2015), and applied in one of the mooring models.

3. Materials and methodology

3.1. PC semi materials

The materials required for the design of the PC Semi are primarily steel. However, other structures like the composite marine risers, bonded marine hoses, and mooring lines have different materials like composites (Amaechi et al., 2017, 2019c; 2019d; 2019e; 2019f) and polyesters (Amaechi et al., 2021a, 2021b; 2021c). It is noteworthy that some of the materials obtained from the study on the mass calibration in Table 6 were classified as '*additional mass*', as detailed in earlier study (Odijie, 2016; Odijie et al., 2017b). Materials such as the weight of ballast liquid and riser liquid are considered as an additional mass. In this study, the value for additional mass was varied according to the functionality, applicability, and purpose of design for the hull of the PCSemi. Fig. 5 shows the structure with detail of the topside and mezzanine deck.

3.2. Mooring materials

The material selection is an essential aspect of the mooring design as polyesters, composites, and steel all have varying material properties (Ye et al., 2020; Amaechi C.V. et al., 2019e, 201f). The mooring lines are made up of mainly two materials in the configuration-steel and polyester. Steel material was used in constructing the PCSemi hull, similar to the other validated PCSemi studies (Odijie et al., 2015, 2017b; Bhosale, 2017; Odijie, 2016). It was also used in the design of the Steel Catenary Risers (SCR) and Top Tension Risers (TTR), the chain mooring lines,

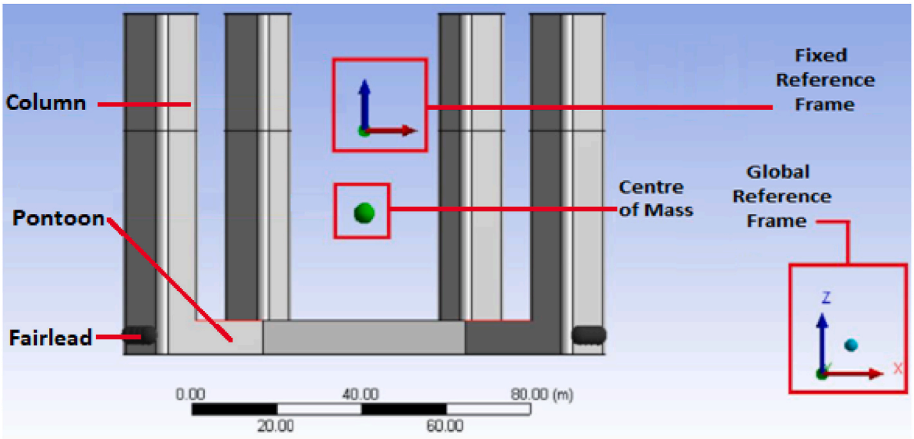

Fig. 11. Front view of PC Semi hull showing fixed and global reference frames (in ANSYS AQWA R2 2020).

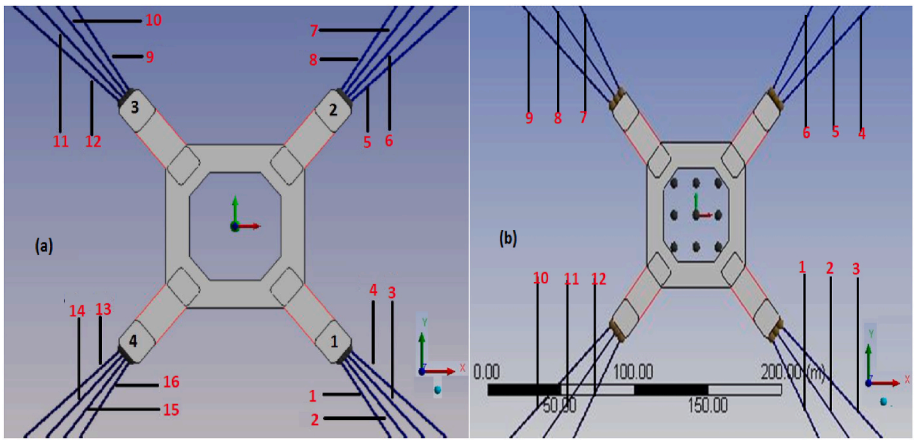

Fig. 12. The Numberings for two Mooring Configurations on the PCSemi Columns, showing (a) 16 mooring lines and (b) 12 mooring lines (in ANSYS AQWA R2 2020).

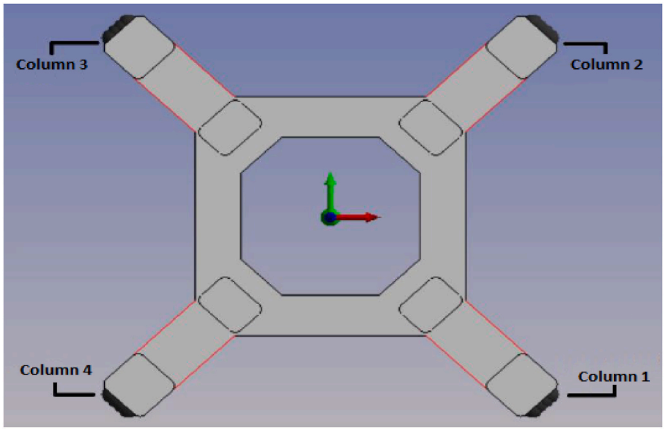

Fig. 13. Configuration of PCSemi hull (in ANSYS AQWA R2 2020).

Table 4
Fixed Point for the mooring lines on the anchor of PC Semi Hull.

Fixed Point	X (m)	Y (m)	Z (m)
1	1979.3	−1527.3	−2385.035
2	1841.7	−1690.6	−2385.035
3	1527.3	−1979.3	−2385.035
4	1690.6	−1841.7	−2385.035
5	1979.3	1527.3	−2385.035
6	1841.7	1690.6	−2385.035
7	1527.3	1979.3	−2385.035
8	1690.6	1841.7	−2385.035
9	−1979.3	1527.3	−2385.035
10	−1841.7	1690.6	−2385.035
11	−1527.3	1979.3	−2385.035
12	−1690.6	1841.7	−2385.035
13	−1979.3	−1527.3	−2385.035
14	−1841.7	−1690.6	−2385.035
15	−1527.3	−1979.3	−2385.035
16	−1690.6	−1841.7	−2385.035

Table 3
Connection Point for the mooring lines on the fairlead of PC Semi Hull.

Connection Point	X (m)	Y (m)	Z (m)
1	54.868	−50.625	−48.865
2	53.454	−52.039	−48.865
3	50.625	−54.868	−48.865
4	52.039	−53.454	−48.865
5	54.868	50.625	−48.865
6	53.454	52.039	−48.865
7	50.625	54.868	−48.865
8	52.039	53.454	−48.865
9	−54.868	50.625	−48.865
10	−53.454	52.039	−48.865
11	−50.625	54.868	−48.865
12	−52.039	53.454	−48.865
13	−54.868	−50.625	−48.865
14	−53.454	−52.039	−48.865
15	−50.625	−54.868	−48.865
16	−52.039	−53.454	−48.865

Table 5
Details of mooring azimuths and pretensions in one of the mooring models.

Group No.	Line No.	Azimuth (deg.)	Pretension (kN)
1	1	52.5	2967.0
	2	47.5	2967.0
	3	42.5	2967.0
	4	37.5	2967.0
2	5	322.5	4190.2
	6	317.5	4190.2
	7	312.5	4190.2
	8	307.5	4190.2
3	9	232.5	4070.0
	10	227.5	4070.0
	11	222.5	4070.0
	12	217.5	4070.0
4	13	142.5	2847.0
	14	137.5	2847.0
	15	132.5	2847.0
	16	127.5	2847.0

anchors, fairleads, pontoon, braces, topside deck, and mezzanine deck. The offshore industry recommends between grades 50–80 steel for constructing drilling and production semisubmersible hull systems. The yield stress of this steel grade range is 350 MPa–550 MPa. In this study, the minimal strength was considered at 350 MPa, to ensure a safe design, and details on the properties of the steel material considered are presented in Table 7. In the mooring design, the length of polyester rope was quite lengthy to reduce the dead weight of the mooring lines. The details of all the properties of the chain-polyester-chain mooring line are steel-polyester-steel configuration considered in the mooring design are presented in Table 8. It was modelled by considering two validated PCSemi mooring models (Das and Zou, 2014; Bhosale, 2017), including details for the Maximum Breaking Load (MBL). The polyester rope and steel chains were not experimentally tested here in the present study (see further discussion in Section 3.6). Corrosion allowance was not considered in this study. Fig. 14 is a typical studless R4 mooring chain.

Table 6
Summary of mass calibration.

Mass	Component	Magnitude
Buoyancy	Mass of the displaced water	96.5×10^6 kg
Deck	Facilities and utilities	(25.1–34) x 10^6 kg
Hull steel	Columns, pontoon, braces & internal reinforcement	26.72×10^6 kg
Topside steel	Truss and plate	9.1×10^6 kg
Additional	Ballast liquid, dead oil	$4.5–11.0 \times 10^6$ kg
Attachments	Mooring and Risers	10.1×10^6 kg

Table 7
Properties of steel.

Particulars	Value	Unit
Strength	350	MPa
Density	7850	Kg/m^3
Young's modulus	200	GPa

3.3. Methodology

The methodology considered in the mooring design and the mooring analysis involved using hydrodynamic data from ANSYS AQWA R2 2020 and loading these into Orcaflex 11.0f. Another aspect of the mooring analysis was by classification bases on two classes: similar and dissimilar classifications. In addition to the mooring analysis, the performance evaluation of two different mooring configurations – taut and catenary was also conducted and briefly discussed. Each design config was investigated in three different ways, namely: "Intact Condition", "Damaged Condition" and "No Mooring Cables Attached". In the intact condition, all the mooring lines were attached, whereas the damaged condition is when one mooring cable had been suppressed to investigate the effect of tension on the other mooring lines. In the fully coupled mooring analysis, the irregular wave was applied, and the impact of slow drift has been ignored under Time Domain (TD) and Frequency Domain (FD). In addition, the considerations of number of moorings were also considered. The governing equations used in the calculation of the statics for the mooring lines is the Catenary equation, which is applicable on Steel Catenary Risers (SCR), flexible risers and cable structures (Bai and Bai, 2005; Irvine, 1981). A typical illustration considered for the catenary line in the chain-polyester-chain mooring line configuration is given in Fig. 15. The finite element model of the mooring system in Orcaflex is shown in Fig. 16.

3.4. Hydrostatic stiffness

For rigid body motion analysis, stiffness is a fundamental property required as a boundary condition around the affected area. This study presents the hydrostatic stiffness computed for the PCSemi hull and utilised in the analysis in Table 9. The results of the hydrostatic displacement properties at the Centre of Gravity (CoG), Z of −19.6 m, are given in Table 10.

3.5. Environmental conditions

The PCSemi hull considered in this study was based on environmental conditions in the Gulf of Mexico (GoM), as presented in Tables 11–13. The data was extracted from the interim hurricane guidelines for GoM in API 2INT-MET (API, 2007). The mooring line configuration with 16 moorings, depicted in Fig. 16 (a), was adopted, as it performed better under the different environmental conditions, with similar approaches in the project studies (Odijie, 2016; Bhosale, 2017). Theoretical formulations in earlier sub-sections have shown that motion response can be due to the water particles kinematics in waves, motions of the structure, and the interactions between waves, the risers, and the PCSemi hull. In this study, the environmental conditions are considered as part of the loads (Hirdaris et al., 2014; Odijie et al., 2015, 2017a; Amaechi et al., 2019a, 2019b; 2019c; 2019d). The wave spectrum considered in this study was the JONSWAP (Joint North Sea Wave Project) Spectrum. JONSWAP wave spectrum accounts for any imbalance in the energy flow within the wave system. The JONSWAP spectrum (Hasselmann et al., 1973) was modified from Pierson-Moskowitz spectrum (Pierson and Moskowitz, 1964) to take care of regions that have geographical boundaries so as to limit the fetch as regards the wave generation. In this study, the simulation setup for the numerical model showing the current and wind profiles in ANSYS AQWA R2 2020 is given in Fig. 17.

3.6. Method of analysis

In this investigation, both Orcaflex and ANSYS AQWA were utilised for obtain the results. For clarification, Sections 4.1-4.5 were analysed from ANSYS AQWA while Sections 4.6-4.8 were analysed from Orcaflex 11.0f. Based on the definition of utilised terms, 'Homogeneous' and

Fig. 14. Typical studless R4 mooring chain.

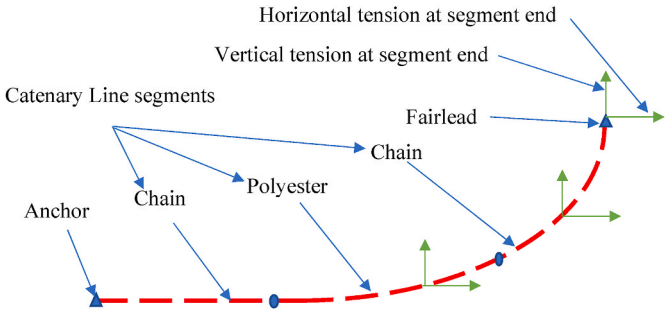

Fig. 15. Typical catenary line considered for chain-polyester-chain mooring line configuration.

Table 8
The composition of the mooring lines.

Item	Description	Diameter (m)	Length (m)	Wet Weight (kg/m)	Maximum Breaking Load, MBL (kN)	Axial Stiffness, EA (kN)
Chain on fairlead	Studless R4	0.1588	140.208	438.90	19,563.30	1,842,397.80
Polyester	Polyester	0.2699	3596.64	12.50	21,351.50	256,217.60
Chain on anchor	Studless R4	0.1588	91.44	438.90	19,563.30	1,842,397.80

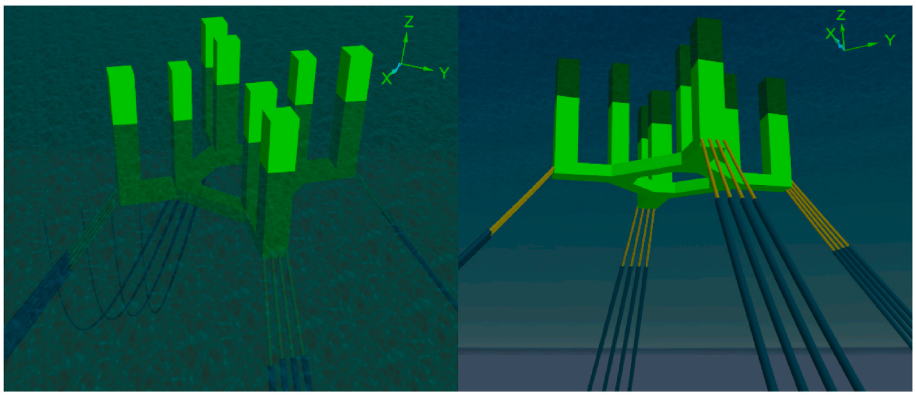

Fig. 16. Finite Element Model of Paired Column Semisubmersible, showing (a) top and (b) underneath views in Orcaflex.

Table 9
Hydrostatic stiffness.

Hydrostatic Stiffness			
	Heave	Roll	Pitch
Heave	12930496N/m	0.7923804N/^{0}	2.2218773N/^{0}
Roll	45.400051N.m/m	1.41608E8N.m/^{0}	46.600529N.m/^{0}
Pitch	127.30419N.m/m	46.600529N.m/^{0}	1.41608E8N.m/^{0}

Table 10
Hydrostatic displacement properties.

Parameters	1st Motion	2nd Motion	3rd Motion
Centre of Buoyancy (COB) Position	X: 4.2791E-5m	Y: 1.5276E-5m	Z: -32.776302 m
Out of Balance Forces/ Weight	FX: -1.8794E-8N	FY: 1.1008E-7N	FZ: 3.6637E-6
Out of Balance Moments/ Weight	MX: -5.4023E-6m	MY: -3.6163E-5m	MZ: -9.3266E-6

Table 11
Parameters for the environmental conditions.

Parameters	Operation condition	Extreme condition	Survival condition
Significant wave height (m)	13.1	15.4	16.4
Maximum wave height (m)	23.1	27.2	28.9
Peak spectral period (s)	15.1	15.8	16.7
Period of maximum wave (s)	13.6	14.2	15.1

NB: γ is the peak enhancement factor where $\gamma = 2.2$; JONSWAP Wave Spectrum;

Table 12
Parameters for current.

Parameters	Operation condition	Extreme condition	Survival condition
Current at 0 m depth (m/s)	1.91	2.38	2.49
Current at 50 m depth (m/s)	1.43	1.79	1.87
Current at 100 m depth (m/s)	0	0	0.1
Current at 2,400 m depth (m/s)	0	0	0
0-speed depth	83.8	100.0	104.7

Table 13
Parameters for wind.

Parameters	Operation condition	Extreme condition	Survival condition
1-h mean wind speed	39.9	47.6	49.9
10-min mean wind speed	44.7	54.0	56.8
1-min mean wind speed	50.8	62.2	65.7
3 s Gust wind (m/s)	58.8	72.9	77.3

'Non-Homogeneous' mooring cables are considered in this investigation by considering two models of Chain-Polyester (CP) and Chain-Polyester-Chain (CPC) mooring line configurations. In this investigation, similar mooring system is the homogenous mooring system of Chain-Polyester (CP) mooring configuration. Also, the dissimilar mooring system is the non-homogeneous mooring system of Chain-Polyester-Chain (CPC) mooring line configurations. Furthermore, the response study on the mooring presented in Section 4 was presented under 250s and 500s. These time runs were due to model simplicity and time effectiveness, rather than using longer times of 10,800s (3 h). However, the runs were also compared with the 3 h model and had no change in the effects investigated on the mooring analysis. It should be noted that 3 h gives full run time for fully developed seas. However, the mooring analysis was based on operational comparisons. Thus, using less time saved computational resources for the investigation and simplified the presentation of the output.

In this research, the polyester rope stiffness has been modelled as a constant value of approximately 12 x MBL was considered as it was simulated to be effective for the PCSemi model in Tables 8 and 14. The PCSemi model is much bigger than typical marine Wave Energy Converters (WECs), ocean monitoring devices, or marine breakwater devices. Thus, the mooring requirement uses more length of mooring lines. The dynamic polyester rope stiffness usually varies in the range between 18 x MBL and 35 x MBL. However, that holds mostly on mooring smaller marine energy structures like multi-column WECs (Aggidis and Taylor, 2017; Doyle and Aggidis, 2019, 2021; Falcão, 2010), Oscillating Water Column WECs (Falcão and Henriques, 2016; Heath, 2012), Catenary Anchor Leg Mooring (CALM) buoy systems (Amaechi et al., 2019c, 2019d) and Break water devices (Weller et al., 2013; Wichers, 2013; Bai and Bai, 2005). Although, using the fiber rope mooring analysis procedure recommended in standards like DNVGL-RP-E305 and ABS (ABS, 2021c), the polyester rope stiffness has been modelled as a constant value of approximately 12 x MBL are applied for polyester, which was verified to be working on the validated PCSemi model.

In addition, the experimental investigation on Maximum Breaking Load (MBL) and fatigue analysis on the mooring model were not included in this manuscript but considered in further studies. The min-

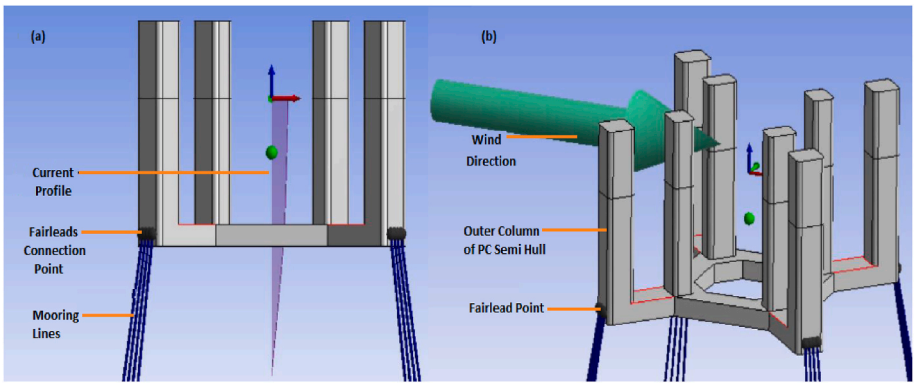

Fig. 17. Simulation setup showing (a) current and (b) wind profiles (in ANSYS AQWA R2 2020).

Table 14
Validation Parameters of Paired Column Semisubmersible model.

Model Parameters	Diameter (m)		Stiffness, EA (N)		Wet Weight (kg/m)		Max Tension (N)	
	Platform Chain	Polyester Rope	Platform Chain	Polyester Rope	Platform Chain	Polyester Rope	Platform Chain	Polyester Rope
RPSEA Model	0.15875	0.26988	1.8E+09	2.6E+08	438.904192	12.5006	2E+07	2.1E+07
Present Model	0.127	0.2731	2.5E+09	1E+08	308.381303	44.078	4433690	1.6E+07

imum breaking strength of polyester fiber ropes are evaluated using either one of the following test procedures: Procedure A is based on the CI Standard 1500-02 or procedure B is based on BS ISO 18692. However, the experimental testing of the fibre rope is also not considered in this investigation. The load at which this occurs is often quoted by rope manufacturers as the Maximum Breaking Load (MBL) and will depend not only on the applied load rate but also the condition of the rope. In terms of strength, the rope that is selected will depend on the expected extreme loads of the mooring system and required safety factor (S.F). The DNV–OS–E301 (DNVGL, 2015) on Position Mooring guideline

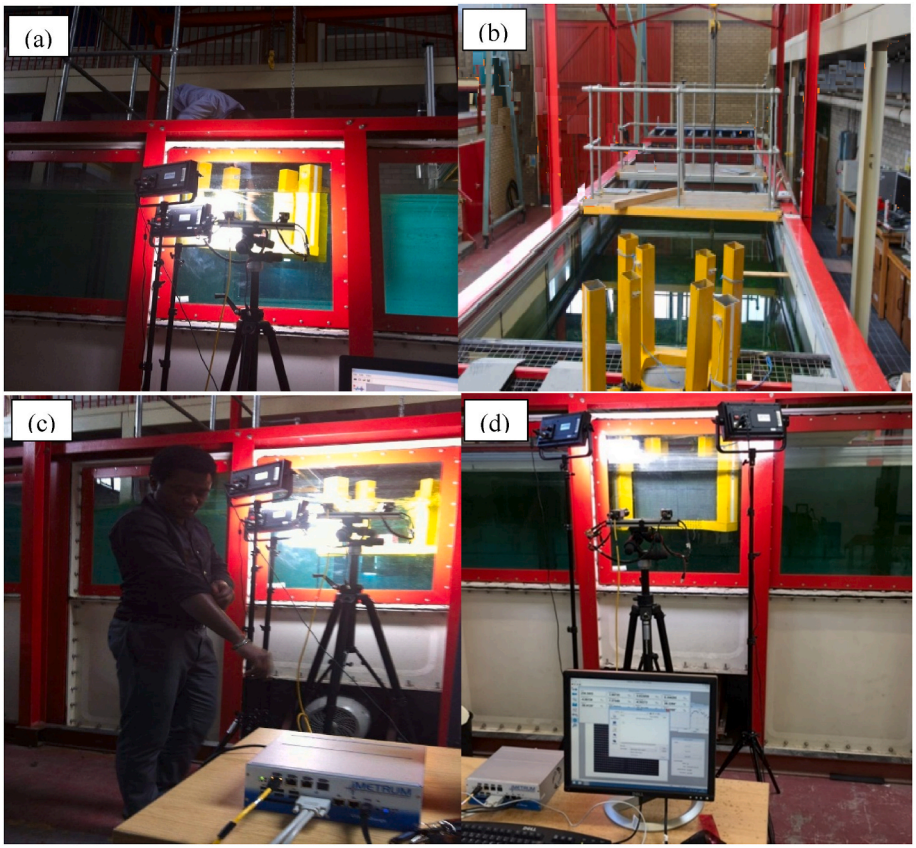

Fig. 18. Experimental study of Paired Column Semi-Submersible, showing (a) Side view of Lancaster University Wave Tank setting up an experiment with the PC Semi Test model, and (b) Right Front view of the Lancaster Wave Tank showing the model test rig, (c) Side view of Lancaster University Wave Tank while setting up the Imetrum Device for the PC Semi Test model, and (d) Side view of the Imetrum Device with camera and high powered lights during data collection.

defines the strength (S_c) of steel wire, chain and synthetic components based on the mean value of breaking strength (μs) and the coefficient of variation of breaking strength (δs):

$$S_c = \mu_s[1 - \delta_s(2 - 6\delta_s)] \quad (2)$$

3.7. Validation

An essential aspect of this investigation is the validation of the numerical model. To ensure that the correct mooring model is being implemented for the analysis, it is crucial to validate the model against a standard. At the time of this study, the fabricated PCSemi model was only tested for motion performance in Lancaster University Wave Tank, conducted using Imetrum system (Imetrum, 2016, 2017, Milad et al., 2018; Aboshio et al., 2015) as shown in Fig. 18. The size of the Lancaster University wave tank facility is 12.5 m in length, 1.7 m in depth and 2.5 m in width. The facility was installed by Edinburg Designs, and it has seven (7) paddles, that generate waves. The wave frequency applied in the wave runs ranged from 0.5 Hz to 1 Hz. From the experimental images, it can be seen that the width of the PCSemi model is almost half of the width of the tank. Since the reflected wave of the lateral wall will significantly influence the motion response of the model, the challenge was removing the reflected waves. In this experiment, the digital image capture (DIC)'s calibrator for the Imetrum system was used to record the motion references through a black background. Also attached to the PCSemi's hull model at one end was a dark board having white dots, as depicted in Fig. 18(d). In addition, the accuracy of the captured data was improved by the use of two (2) high-powered lamps which were focused around the zone of concentration. This experiment was compared with another experiment that was conducted in MARIN's wavetank facility to extract the VIM, however the flow's current, and the backward hydrodynamic reflection for the side wall were not accounted for (RPSEA, 2009, 2014). Details on the method for the removal of the reflected wave from the lateral sides or side walls are presented in literature (Odijie, 2016). Still, the experiment did not include mooring analysis but free-floating and stability. Details of the experimental investigation are available in Odijie (2016) and RPSEA (2009). The numerical model for the PC Semi used in ANSYS AQWA was validated against existing literature (RPSEA, 2009, 2014; Odijie, 2016; Bhosale, 2017; Das and Zou, 2015). Table 14 shows the various setup parameters used in the two models. With limited Company Reports on mooring analysis of Paired-Column Semisubmersible not being readily available, the studies in RPSEA (2009, 2014) had to be used to validate the setup model. The experimental setup in RPSEA (2014a,b) was modelled in ANSYS AQWA for the same conditions, and the results were compared with the findings obtained (see Bhosale, 2017). Models were also developed with the results obtained from experimental response analysis carried out in this research. A mesh study was also done during this process, as presented in Section 2.4. Based on the validation of the model, the comparison was conducted based on the structures' horizontal acceleration response (as in Fig. 19(a)) and vertical acceleration response spectrum (as in Fig. 19 (b)). The results in Fig. 19 agrees fairly between the present data and the RPSEA (2014a,b) study. However, the difference in the size of the wave tanks and the ratio of the model to the wave tank are factors affecting this variation. Note that the setup in Fig. 18 is for PCSemi model without mooring, and not based on the experiment in Fig. 19.

4. Result analysis and discussion

In this section, the mooring analysis was carried out.

4.1. Effect of intact and damaged mooring lines

In this section, the effect of intact mooring lines and damaged mooring lines is investigated under a time response analysis on the PCSemi structure. Different cases were considered using the

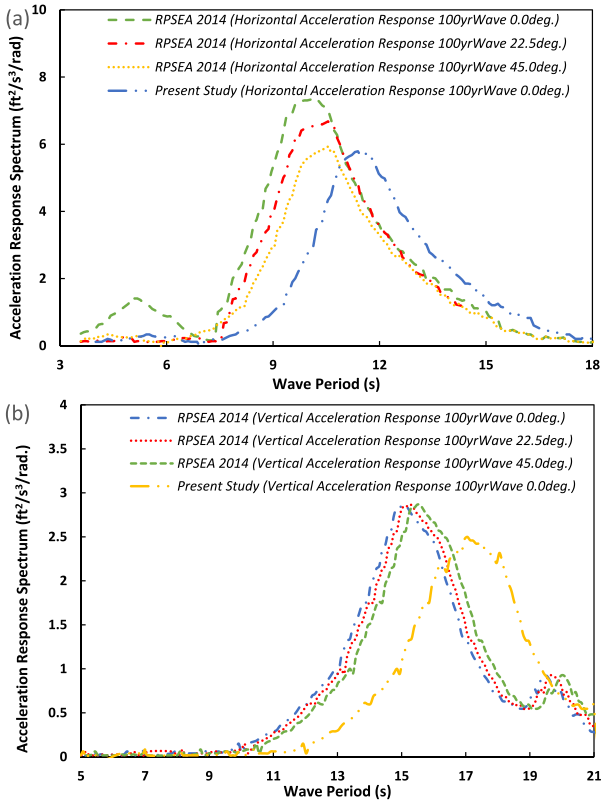

Fig. 19. Validation study for the present study and RPSEA (2014a,b), showing (a) Horizontal Acceleration Response, and (b) Vertical Acceleration Response, both under 100yr wave at location (0.0,0.0.100.0).

environmental conditions in Section 3.5. Since there are no mooring cables on the structure, only the platform is subjected to the environmental forces, and its responses are recorded below. Since the structure is precisely symmetric to the oncoming forces, it does not produce any motions in the yaw, roll and sway directions as this reflects in the motion behaviour. As seen in Table 15, the damaged and intact cases had different effects on the mooring line tension. In Group 4, one of the lines was suppressed as a damaged line in Mooring line 13, as will be discussed subsequently. During the hydrodynamic analysis, the force exerted on the cables showed that the intact cases had higher tensions than the damaged ones. In addition, it can be observed that the case of Chain-Polyester-Chain (CPC) had higher tensions than the Polyester-Polyester (PP) configurations, which will be due to the stiffness of the materials. As such, the CPC configuration performed better and is more reliable for the paired column semisubmersible, and is recommended.

4.2. Effect of different mooring cases on wave spectra

The effect of different mooring cases was investigated under the PCSemi mooring system under the catenary mooring system in deep water conditions. The results in Fig. 20 evaluates the performance of the similar and dissimilar Mooring Lines. As can be observed in Fig. 20(a), mooring line 13 (ML13) was the damaged case, and the spectral density reflects a shift in the wave spectra, unlike those of the mooring lines 14–16 (ML14, ML15, ML16) that are much closer to one another. In Fig. 20(b) and (c), the intact and damaged cases show that both the chain-polyester-chain and the polyester-polyester configurations are very similar and close to one another. Still, the latter has a bit higher spectral density, since it involves lighter materials. In Fig. 20(d), when there are no moorings attached, the wave spectra for the also similar but have wider dispersion between each configuration investigated. Thus, this shows that the material used in mooring lines have an influence on

Table 15
Maximum Tension Values in CPC and CP Configurations for Intact and Damaged condition.

Group No.	Mooring Line	Chain-Polyester-Chain (CPC) Configuration		Polyester-Polyester (PP) Configuration	
		Max. Tension (kN) Intact Line	Max. Tension (kN) Damaged Line	Max. Tension (kN) Intact Line	Max. Tension (kN) Damaged Line
1	1	2289.09	2279.75	1576.50	1570.97
	2	2285.85	2279.15	1570.80	1568.66
	3	2277.42	2279.13	1559.78	1564.42
	4	2281.92	2279.22	1565.29	1567.28
2	5	2272.53	2278.38	1502.65	1527.24
	6	2270.77	2273.67	1500.92	1520.92
	7	2266.89	2263.92	1499.77	1510.58
	8	2268.78	2269.07	1500.33	1515.39
3	9	2288.47	2251.96	1576.46	1543.46
	10	2285.03	2248.29	1570.78	1539.47
	11	2277.09	2242.81	1559.33	1529.11
	12	2281.34	2246.89	1564.86	1533.62
4	13	2273.01	DAMAGED	1502.62	DAMAGED
	14	2270.44	2305.36	1501.36	1557.29
	15	2266.59	2300.77	1500.23	1552.29
	16	2267.98	2303.43	1500.47	1554.80

the PCSemi. It should be noted that the response in Fig. 20 (a-d) is also subject to the natural frequency of the PCSemi system considered.

In Fig. 20(a), Although the response amplitude almost appears not to show changes in the wave spectra in the mooring line 13 damaged case, there are changes. The apparent small changes in the wave spectra is due to the runtime been 250s, which meant lesser time. Under a longer runtime of up to 3 h (10,800s) for fully developed flows would reflect a much higher difference in amplitudes on the wave spectra. Also, the natural frequency of the PCSemi system shown in Fig. 20(d) appears to keep basically the same with the other three conditions including the effects of mooring, but they are different in the wave spectra at peaks of 89.88 m^2/Hz and 91.49 m^2/Hz, as seen on the gridlines in the spectral density plot, conducted under a shorter time run of 250s, as it shows wider disparities. Thus, the need to investigate the influence of stiffness of the mooring line on the PCSemi mooring system in subsequent section. Secondly, when one of the mooring lines is damaged, the response amplitude of the hull changes. This change might be small, but it depends on the loads on the structure (Hirdaris S.E. et al., 2014; Pimenta, F. et al., 2020; Sarpkaya T.S. 2010) and the type of mooring system considered (Wilson J. 2008; Bai and Bai, 2005; Wichers J. 2013). Since this is not a taut mooring system but a catenary mooring system, as depicted in Fig. 1, it will change. Thus, the reason for the offset as seen in Fig. 20, because the moorings help to offset some of the displacement in the model. Thirdly, the disparity observed between ML13 from other lines ML14, ML15, and ML16 occur when the model is not fully integrated (see similar studies: Azcona et al., 2017; Kim et al., 2018; Sevan-Camas et al., 2018). Another reason is different bending and axial stiffnesses for the moorings, as in the dissimilar mooring cases (see similar studies: Loukogeorgaki and Angelides, 2005, Davies et al., 2008, Odijie et al., 2017b, Das and Zou, 2015).

4.3. *Effect of mooring configurations on mooring tensions*

The effect of the mooring configurations was also investigated on the mooring analysis by considering the maximum tensions obtains for the two mooring configurations, presented in Table 16. Cable Stiffness is another critical parameter that influences the behaviour of the structure in the cases herein. It was observed that the maximum tensions obtained on each group of the mooring line had a different maximum tension profile as observed in Figs. 21 and 22. It is evident that the chain-polyester-chain mooring configuration had higher tensions in all 4 Mooring Groups, than that of the polyester-polyester mooring configuration. This also gives credence to the efficiency of the chain-polyester-chain mooring configuration which has been adopted. The primary concern of any offshore design and this particular design of the mooring system for this PCSemi offshore structure is to ensure that the structure

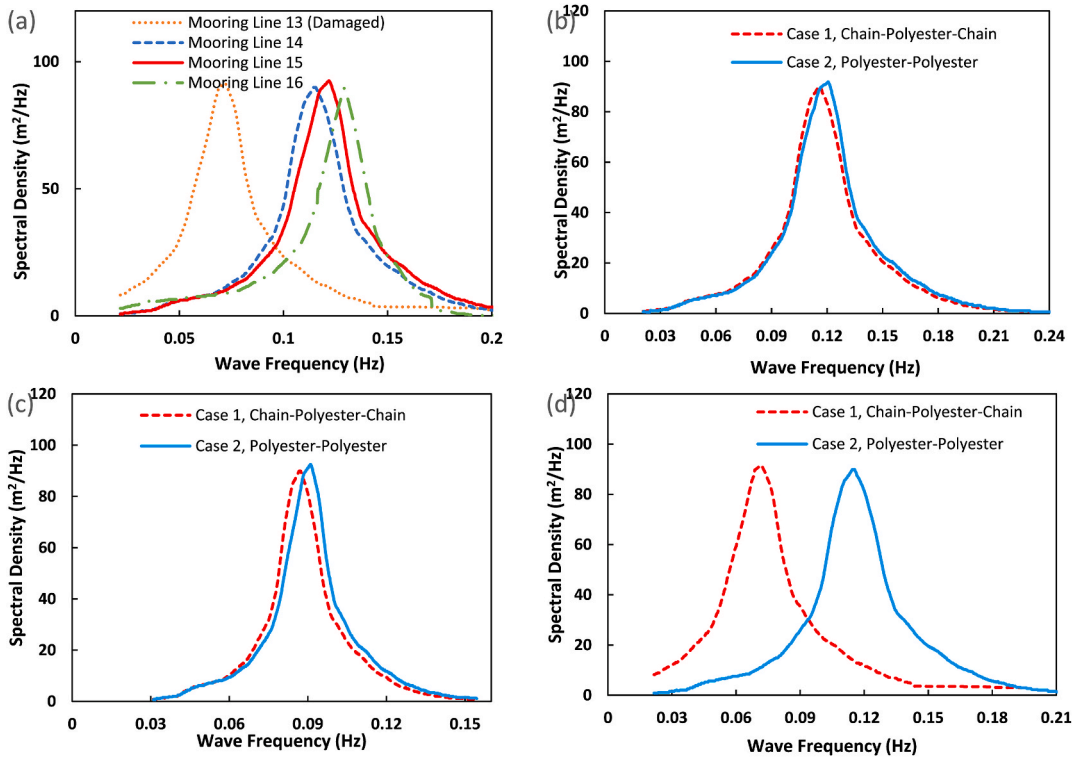

Fig. 20. Wave spectra of chain-polyester-chain and polyester-polyester mooring line configurations, showing (a) one damaged line in Group 4, (b) intact cables, (c) damaged cables, and (d) no mooring cables.

Table 16
The Maximum Tensions for the two Mooring line Configurations.

Groups	Mooring line	Chain-Polyester-Chain	Polyester-Polyester
		Max. Tension (kN)	Max. Tension (kN)
1	1	2289.09	1576.50
	2	2285.83	1570.80
	3	2277.42	1559.78
	4	2281.92	1565.28
2	5	2272.53	1502.65
	6	2270.77	1500.92
	7	2266.89	1499.77
	8	2268.78	1500.33
3	9	2288.47	1576.46
	10	2285.03	1570.78
	11	2277.09	1559.33
	12	2281.34	1564.86
4	13	2273.00	1502.62
	14	2270.44	1501.36
	15	2266.59	1500.23
	16	2267.98	1500.47

remains stable even if one of the cables attached to the structure fails or is damaged. Thus, the need for investigating the different case scenarios that can occur on the structure. In this case, Mooring line 13 (ML13) was chosen randomly to be considered in the damaged case, as the choice is not in any particular industry specification. However, it is recommended that this should be considered and included in industry standards for mooring analysis. In this model, the cable was suppressed, and the platform was subjected to the external forces. In the similar Mooring System that was homogenous, all the mooring lines experienced a higher value of tension when ML13 was suppressed. Whereas in the dissimilar or non-homogeneous mooring system, it was noticed that only the cables on columns 1 and 2 face a higher tension force, and conversely, column 3 and column 4 cables face reduced tension, as presented earlier in Section 4.2.

4.4. Effect of mooring configuration on low-frequency motion

The effect of the mooring configuration on platform low-frequency motion was also investigated on the PCSemi model, as it helped assess the behaviour of the two sets of cables. It can be observed on the six motions investigated that the two configurations have very close effects but not the same result. In Fig. 23(a), the chain-polyester-chain (CPC) configuration had lower surge displacement at 80 m, while the polyester-polyester (PP) configuration had higher surge displacement at 96 m. In Fig. 23(b), the CPC configuration had lower sway displacement at 0.33 m, while the PP configuration had higher surge displacement at 0.38 m. For the heave motion in Fig. 23(c), the PP configuration had higher heave displacement than the CPC configuration. For the rotational motion, there is a similar behaviour between these responses as both configurations had higher oscillation amplitudes in the roll motion in Fig. 23(d). This response behaviour implies that the mooring configuration can affect the stability of the PCSemi. In Fig. 23(a–f), it can be seen that the PP configuration has a lighter density in its response. It can be seen that the pitch motion in Fig. 23(e) has a higher pitch response than the CPC configuration. Also, in the yaw motion in Fig. 23 (f), the response of the PP configuration is relative to the CPC configuration. Also, the PP configuration has a lower amplitude than the CPC configuration in the yaw motion.

4.5. Effect of mooring configuration on wave frequency motion

The effect of the mooring configuration on platform wave frequency motion was also investigated on the PC Semi model, as it was useful in the assessment of the behaviour of the two sets of cables. It can be observed on the six motions investigated that the two configurations have very similar behaviours in Fig. 24(a–f). There is a similar behaviour between the surge and sway motions but different displacements observed, as seen in Fig. 24(a–b). In Fig. 24(a), the chain-polyester-chain configuration had slightly lower surge displacement than the polyester-polyester configuration, and similarly for the sway displacements in Fig. 24(b).

This behaviour is also due to the external forces which are unidirectional and act towards the positive X-axis. Hence, the structure's sway, roll, and yaw show very little motion compared to the surge, heave, and pitch motions. The Chain-Polyester-Chain (CPC) Configuration has a higher overall stiffness in contrast to Polyester-Polyester (PP) Cables. Therefore, the CPC configuration has a smaller amplitude for platform motions in comparison to PP configuration. Although, the PP cable makes up for its low stiffness by having more elasticity as the PP cables experience less tension. For the rotational motion, there is a similar behaviour between these. Both had higher oscillation amplitudes

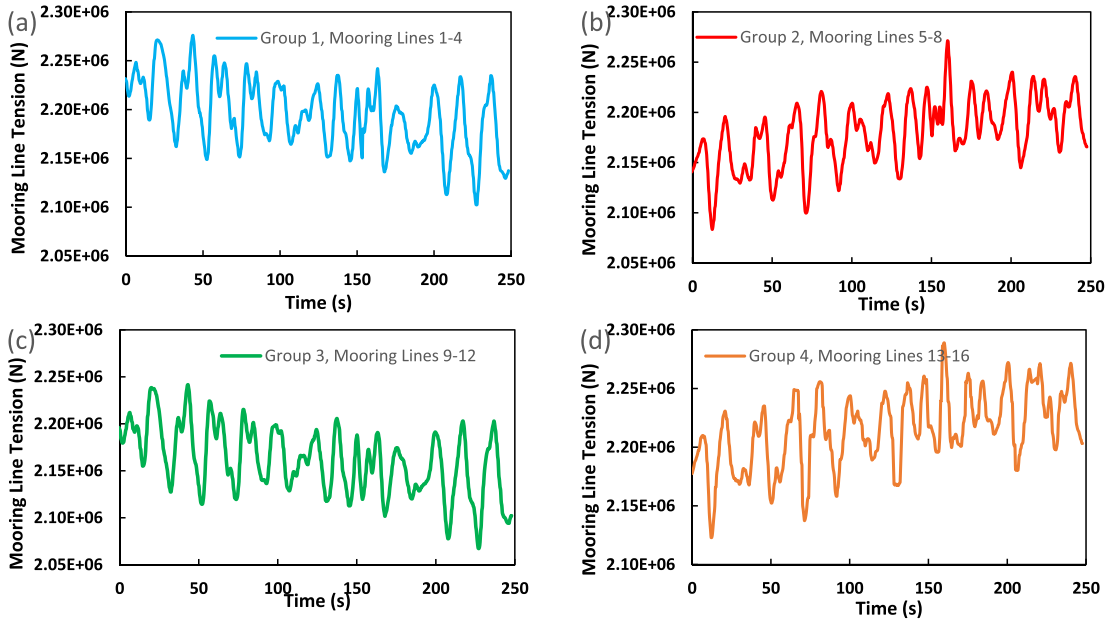

Fig. 21. The mooring line tensions for Groups 1–4 for the PC Semi in Chain-Polyester-Chain Configuration.

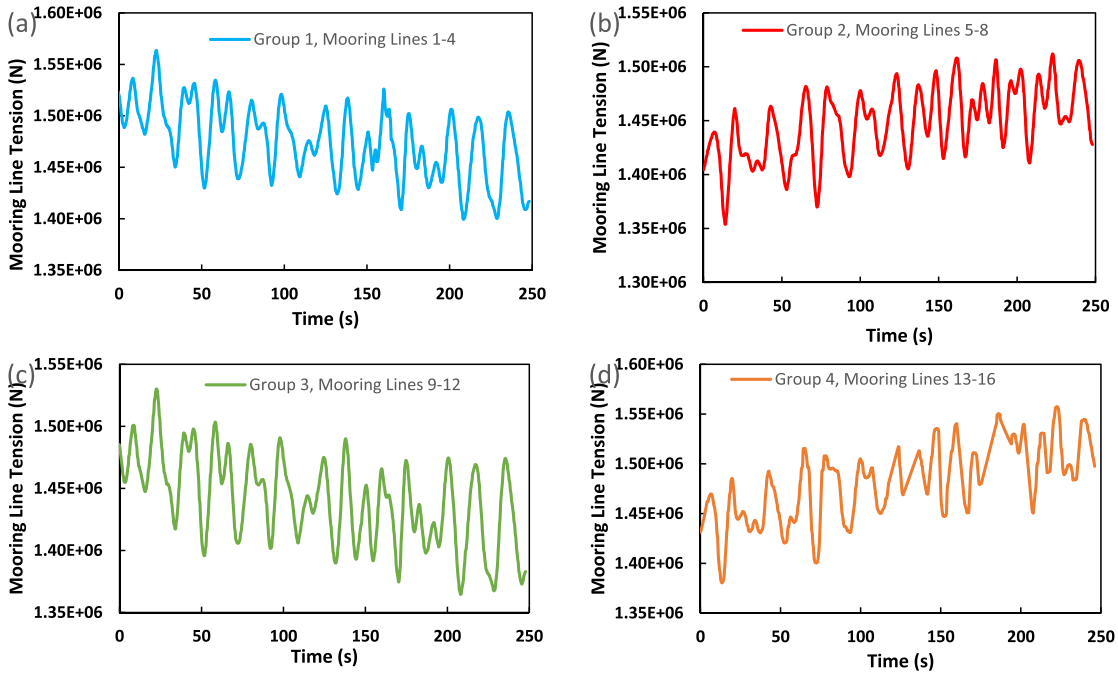

Fig. 22. The mooring line tensions for Groups 1–4 for the PCSemi in Polyester-Polyester configuration.

in the roll motion in Fig. 24(d). Thus, it implies that the mooring configuration can affect the stability of the PCSemi.

4.6. Time response in translational motion

For the translational motion in this study, a time history analysis has been conducted as real-time for two cases: (a) 500 s and (b) 100 s. The time step of 0.01 s for 100 maximum number of iterations were considered for both cases. The motion of the PCSemi was recorded and analysed in the translational motion, as given in Figs. 25–27. It can be observed that both cases have similar behaviour and are almost identical. Thus, they will have a similar wave effect on the hull of the PCSemi, based on the material properties in Section 3.1. It has also been observed that the wave angles affect the time response of the PCSemi motion, as seen in Fig. 25 (b)–(e). The angles were in phases from 0° to 180° in 30-degree intervals for the surge motion. Figs. 25(c), 26(c) and 27(c) present a clearer view of the phase differences for the translational motion in XY plane. Therefore, it is crucial to consider the wave effect based on the wave angles in the stability computation of floating platforms. Based on the sway response, the 0° and 180° cases have the same amplitude and no effect, while others are in phases. The motion is not significant in the 0° and 180° cases, as was observed. Thus, it can be concluded that the sway motion is not very substantial based on phase angles, unlike the surge and heave motions. However, it does present some effects based on the wave angle. For the heave motion, it is evident that the wave angles are in phase of one another, meaning that they follow each other, from 0°, 30°, …up to 180°. It can also be seen that the heave motion is very significant and has almost the same effect for all the angles, as seen in Fig. 26. This difference is virtually similar in the time response plots for the case 60° and case 150° respectively on Fig. 25 (d–e), 26 (d-e) and 27 (d-e).

4.7. Time response in rotational motion

For the rotational motion in this study, a time history analysis has also been conducted as a real-time for two cases: (a) 500 s and (b) 100 s. The time step of 0.01 s for 100 maximum iterations was considered for both cases. The motion of the PCSemi was recorded and analysed in the rotational motion, as given in Figs. 28–30. It can be observed that both cases have similar behaviour and are almost identical. It has also been observed that the wave angles affect the time response of the PCSemi motion, as seen in Fig. 28 (b)–(e). For the rotational motions, the angles were in phases from 0° to 180° in an interval of 30°. The pitch motion has the highest significance on the motion response of the PCSemi. However, this is partly contrary to the roll motion, which is not very significant for cases 0° and 180°, since they are both on the same flat amplitude, thus does not have any effect on the PCSemi hull. For the yaw motion, the cases 0°, 90° and 180° are also on the same flat amplitude. Thus the yaw motion is the least significant of these three (3) rotational motions of the floating paired column semisubmersible. Figs. 28(c), 29 (c) and 30(c) present a clearer view of the phase differences for the rotational motions. Hence, it is vital to consider the wave effect based on the wave angles in the stability computation of floating platforms. In conclusion, the yaw motion is not very significant based on phase angles, unlike the roll and pitch motions. However, it does present some effects based on the wave angle. For the pitch motion, it is evident that the wave angles are in-phase with one another, as they steadily follow each other, from 0°, 30°, …to 180°. It can also be observed that the pitch motion is very significant and has almost the same effect for all the angles, as seen in Fig. 29. This difference is virtually similar in the time response plots for the case 60° and case 150° respectively on Fig. 28(d–e), 29(d-e) and 30(d-e).

4.8. Natural period and natural frequency of PCSemi

The natural period of the Paired Column Semisubmersible was also computed in this investigation. The heave RAO of the PCSemi in Fig. 31 shows that it is subject to different draft sizes. To evaluate the natural period and natural frequency of the PCSemi, a comparative investigation was conducted using earlier studies on this PCSemi model. Since hull movement develops as wave amplitude increases, maximal oscillations are usually measured at resonance frequency. The PCSemi has been developed to work with natural periods that are far apart from the wave's oscillation period, as with other semisubmersibles (Odijie et al., 2017a; Odijie, 2016). Based on the current study, the heave natural periods, Tn are 22.01s (Odijie et al. (2017a, 2017b) and 20.3s (in the

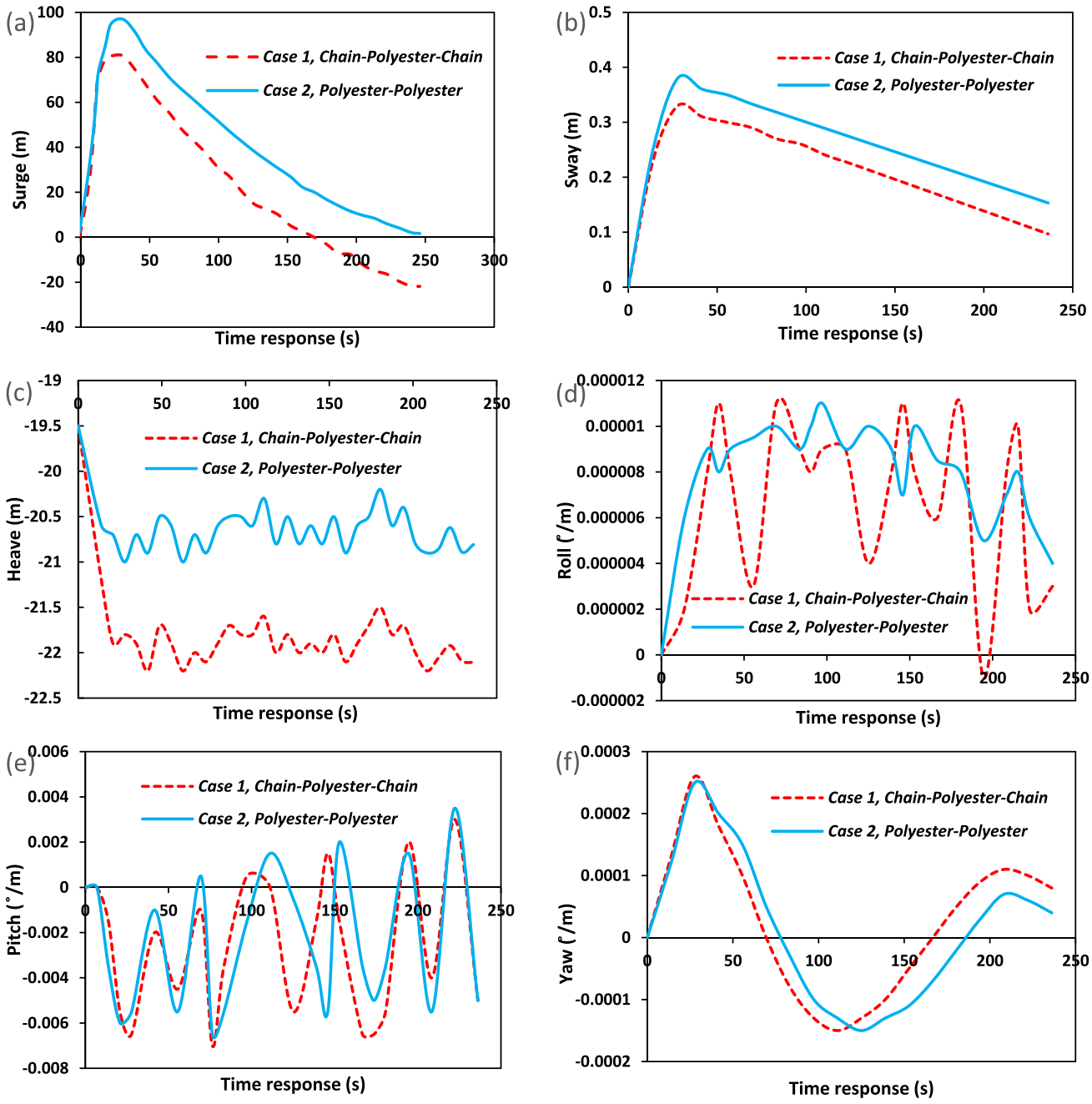

Fig. 23. The response of the Paired Column Semisubmersible for low frequency motion.

present study), also included in the comparative analysis of the heave motion of Paired Column semisubmersible hull in Fig. 32. In the present study, deep draught semisubmersibles' natural periods in each DoF are designed to operate outside of this range. Tsunamis had previously been documented with extremely long periods (near to 21s), although not in deep sea. The natural periods calculated from a decaying test of traditional deep draught semisubmersibles utilised in the GoM were presented by Hussain et al. (2009). The natural periods for pitch, roll and heave motions were 27.3s, 28.4s and 20.0s, respectively. The heaviest natural periods for various draught instances along the heave motion ranged from 21s to 22s. The maximal wave periods measured by weather buoys and the heave natural periods of recently built semisubmersibles are shown in Fig. 32. For example, Matos et al. (2011) provided the specifications of the Petrobras-52 deep draught semisubmersible hull and found that the natural oscillation periods of its heave, roll, and pitch DoF were 23.7s, 33.0s, and 31.5s, respectively. The natural heave period of the hull was given as 20.5s in the prototype of the Glomar Artic 3 semisubmersible provided by Wu et al. (1997). Tan et al. (2016) proposed a model of a deep draught semisubmersible with heave and vortex suppression. The hull was built with a 19.1s heave natural period and 29.4s and 29.3s roll and pitch DoFs, respectively. It also gave the natural periods for heave, roll, and pitch for conventional semisubmersibles in Southeast Asia as 18.4s, 25.8s, and 25.8s, respectively. According to ocean research specifications in publications like the API2INT-MET (API, 2007) obtained via weather buoys to record wave characteristics, the wave durations is between 1s and 17.2s for the operational range of hurricane conditions during 1000-year or 100-year. Thus, as seen in this study, the response of the moorings are within this range.

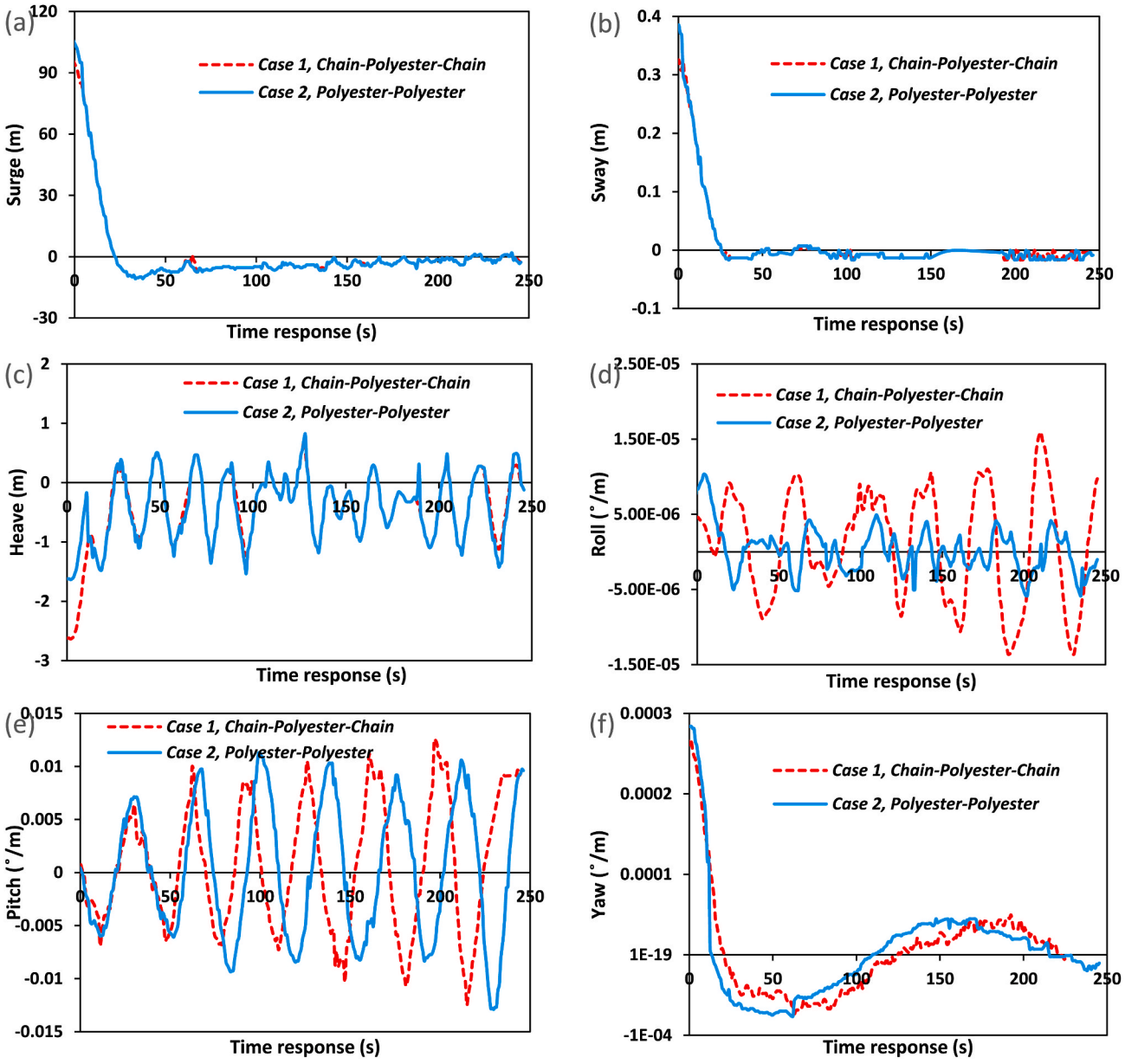

Fig. 24. The response of the Paired Column Semisubmersible for wave frequency motion.

4.9. Discussion

The numerical modelling of mooring line analysis for a novel Paired Column Semisubmersible platform has been conducted in this research. The results of two configurations analysed are presented, along with the motion responses of the structure.

Based on this study, the following discussions and observations were made:

1) A detailed study of the mooring analysis for the effect of intact and damaged mooring lines was presented in Table 15. It showed that the damaged and intact cases had a different impact on the mooring line tension. During the hydrodynamic analysis, the force exerted on the cables showed that the intact cases had higher tensions than the damaged ones. In addition, it can be observed that the Chain-Polyester-Chain (CPC) configuration had higher tensions than the Polyester-Polyester (PP) configurations, which will be due to the stiffness of the materials. Hence, the CPC configuration performed better and is more reliable for the paired column semisubmersible and recommended. However, further study can be carried on the reliability analysis to evaluate the behaviour of the mooring lines in damage conditions.
2) The effect of different mooring cases was investigated on the PC Semi mooring system under catenary mooring system in deep water conditions. The results in Fig. 20 evaluates the performance of the similar and dissimilar Mooring Lines. As can be observed in Fig. 20 (a), mooring line 13 was the damaged case, and the spectral density reflects a shift in the wave spectra, unlike those of the mooring lines 14–16 that are much closer to one another. In Fig. 20(d), when there are no moorings attached, the wave spectra for the also similar but have wider dispersion between each configuration investigated. Thus, this shows that the material used in mooring lines has an influence on the paired column semisubmersible. Further studies are recommended on Maximum Breaking Load (MBL) and fatigue analysis of the mooring system.
3) The effect of the mooring configurations was also investigated on the mooring analysis by considering the maximum tensions obtains for the two mooring configurations, presented in Table 16. Cable

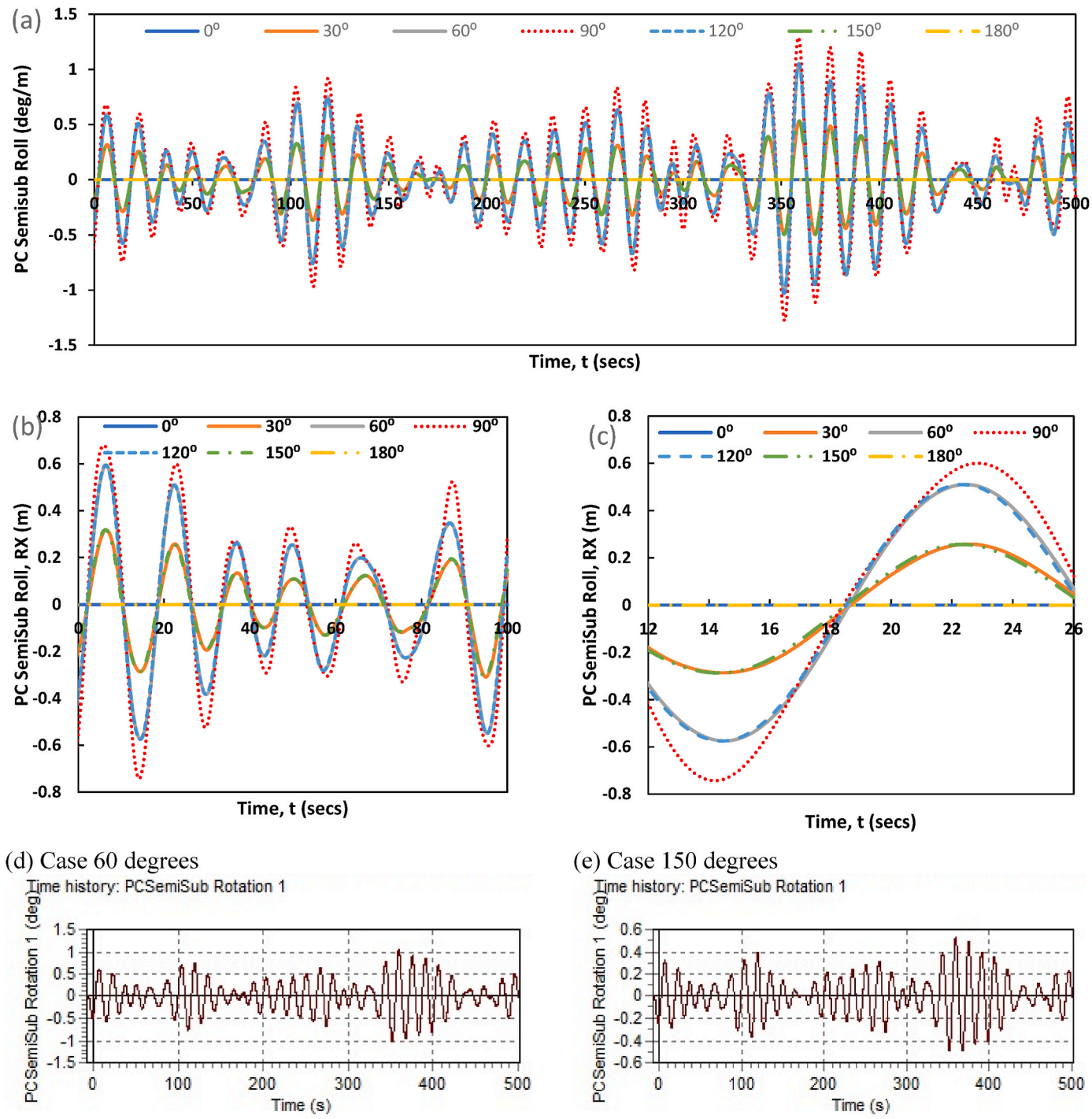

Fig. 25. Surge response of the Paired Column Semisubmersible.

Stiffness is another critical parameter that influences the behaviour of the structure in the cases herein. It can be seen that the maximum tensions obtained on each group of the mooring line had a different maximum tension profile, as observed in Figs. 21 and 22. The chain-polyester-chain mooring configuration had higher tensions in all 4 Mooring Groups, than that of the polyester-polyester mooring configuration. This study also gives credence to the efficiency of the chain-polyester-chain mooring configuration, as was adopted.

4) From the mooring lines study, some similarities in mooring lines patterns are in each mooring group, as in Group 1 (Mooring Lines 1–4), Group 2 (Mooring Lines 5–8), Group 3 (Mooring Lines 9–12), and Group 4 (Mooring Lines 13–16). In this case, Mooring line 13 was chosen randomly to be considered in the damaged case, as the choice is not in any industry specification. However, it is recommended that this should be considered and included in industry standards for mooring analysis. In this model, the cable was suppressed, and the platform was subjected to external forces. In the similar Mooring System that was homogenous, all the mooring lines experience a higher value of tension when Mooring line 13 was suppressed. Whereas in the dissimilar or non-homogeneous mooring system, it was noticed that only the cables on columns 1 and 2 face a higher tension force, and surprisingly column 3 and column 4 cables experience reduced tension. Further study is recommended on the coupling effect of marine risers and the mooring lines.

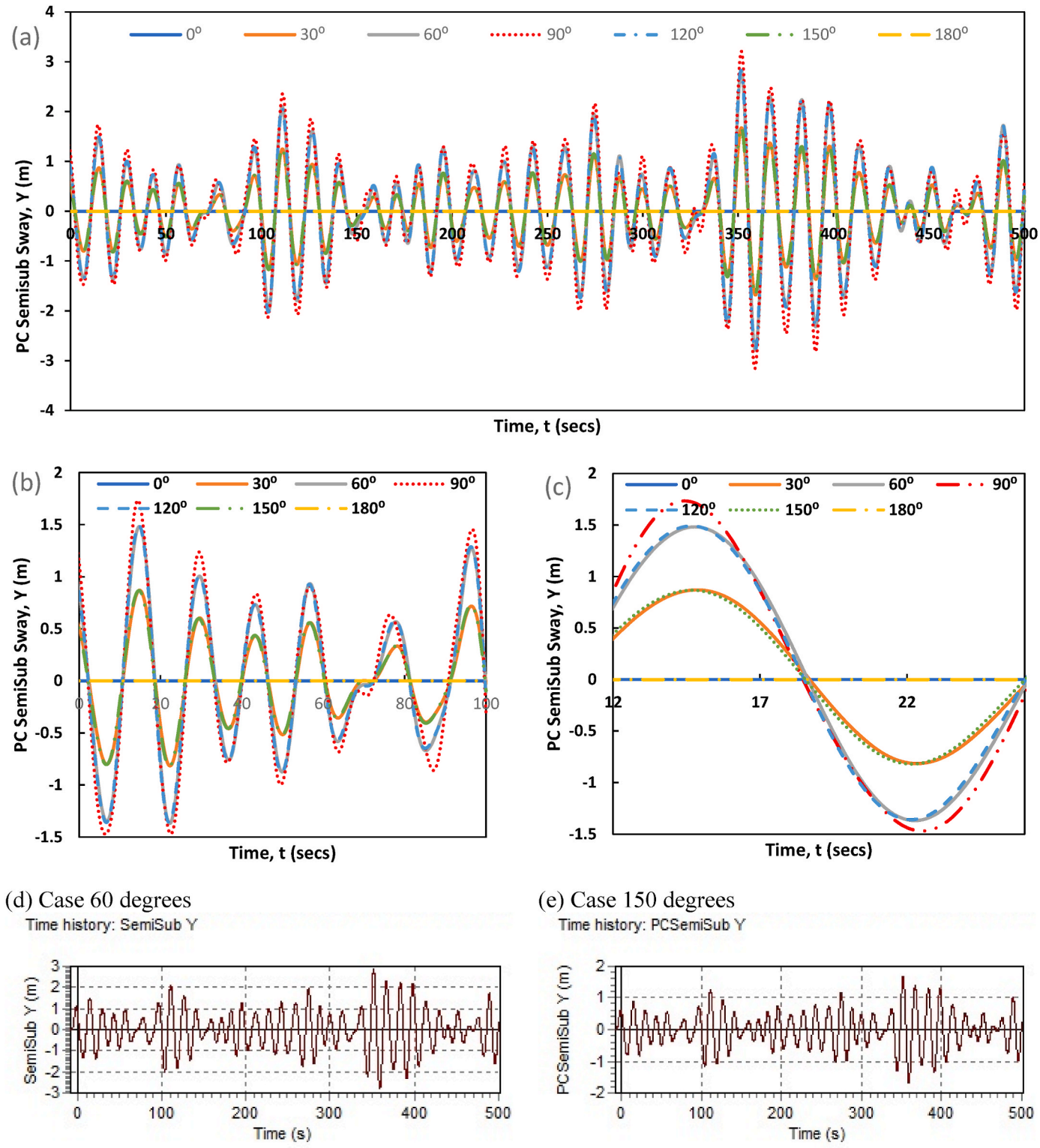

Fig. 26. Sway response of the Paired Column Semisubmersible.

5) It can be observed that the Chain-Polyester-Chain (CPC) Configuration has a higher overall stiffness in comparison to Polyester-Polyester (PP) Cables. Thus, the CPC configuration has a smaller amplitude for platform motions in contrast to PP mooring lines. However, the PP cable makes up for its low stiffness by having more elasticity as the PP cables experience less tension. Further study on damping effect provided from risers on the PC Semi and on the mooring lines.

6) The effect of the mooring configuration on platform low-frequency motion was also investigated on the PC Semi model, as it helped assess the behaviour of the two sets of cables. It can be observed on the six motions investigated that the two configurations have very close effects but not the same effect. In Fig. 24(a), the chain-polyester-chain configuration had lower surge displacement at 80 m, while the polyester-polyester configuration had higher surge displacement at 96 m. For the rotational motion, there is a similar

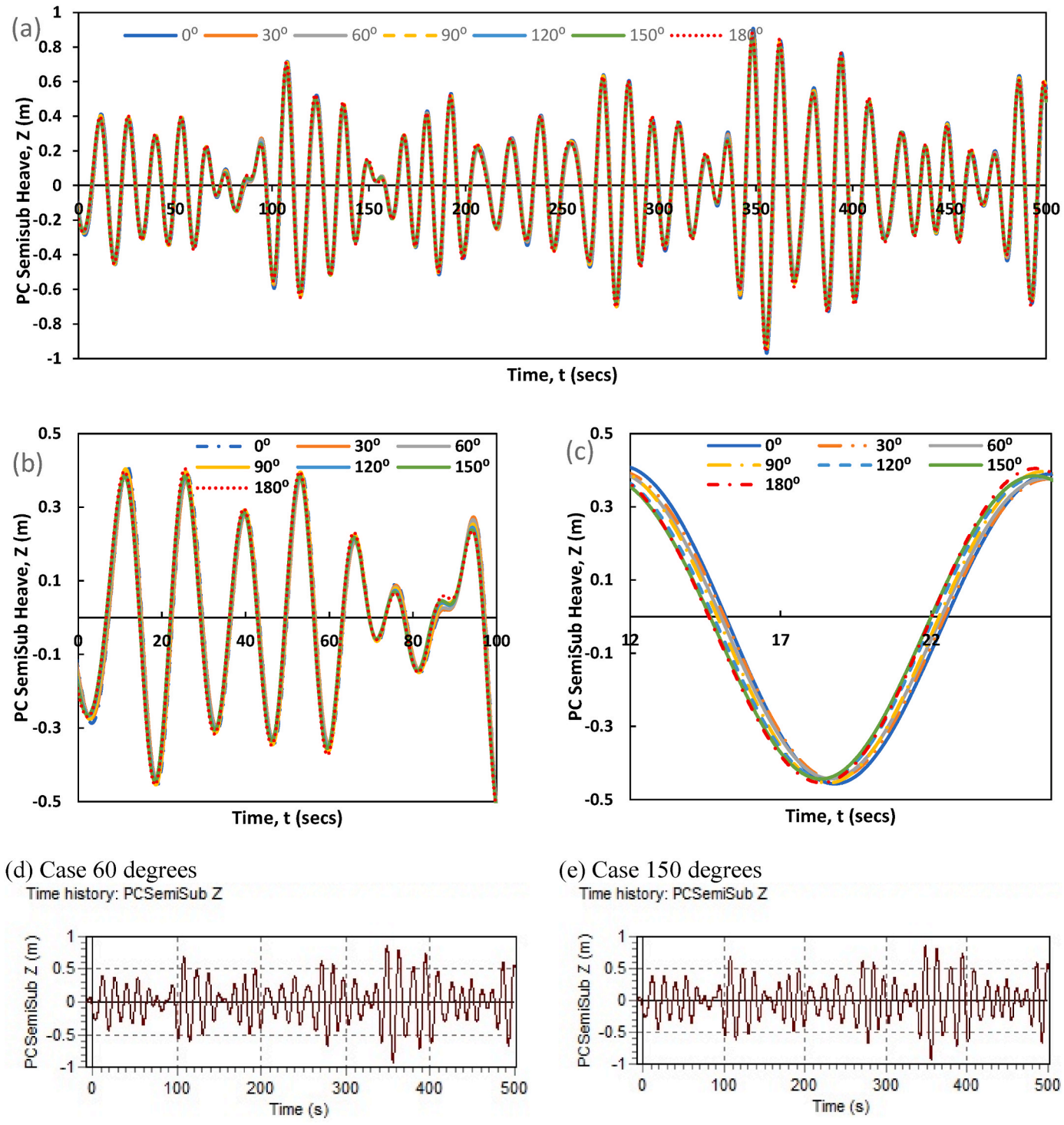

Fig. 27. Heave response of the Paired Column Semisubmersible.

behaviour between these. Both had higher oscillation amplitudes in the roll motion in Fig. 24(d). This implies that the mooring configuration can affect the stability of the PC Semi. Further study can include Dynamic positioning (D.P) used as well as mooring lines to keep the rig in place.

7) By considering the wave headings such as 0°, 15°, 30°, and 45°, it was observed that the angles influenced the global performance of the PCSemi as presented in Sections 4.6 and 4.7. The RAO plots show identical behaviour for the inline flows and similar identical behaviour for the cross flows, which is due to the symmetric nature of the semisubmersible by considering its hull configuration. The RAO plots from the present study perform better in its motion characteristics than a conventional four column semisubmersible with shallower draft size. However, further investigation on the flow behaviour using experiment and CFD is recommended.

5. Conclusion

The numerical study presented is on mooring analysis on the global performance of the paired column semisubmersible in deep water

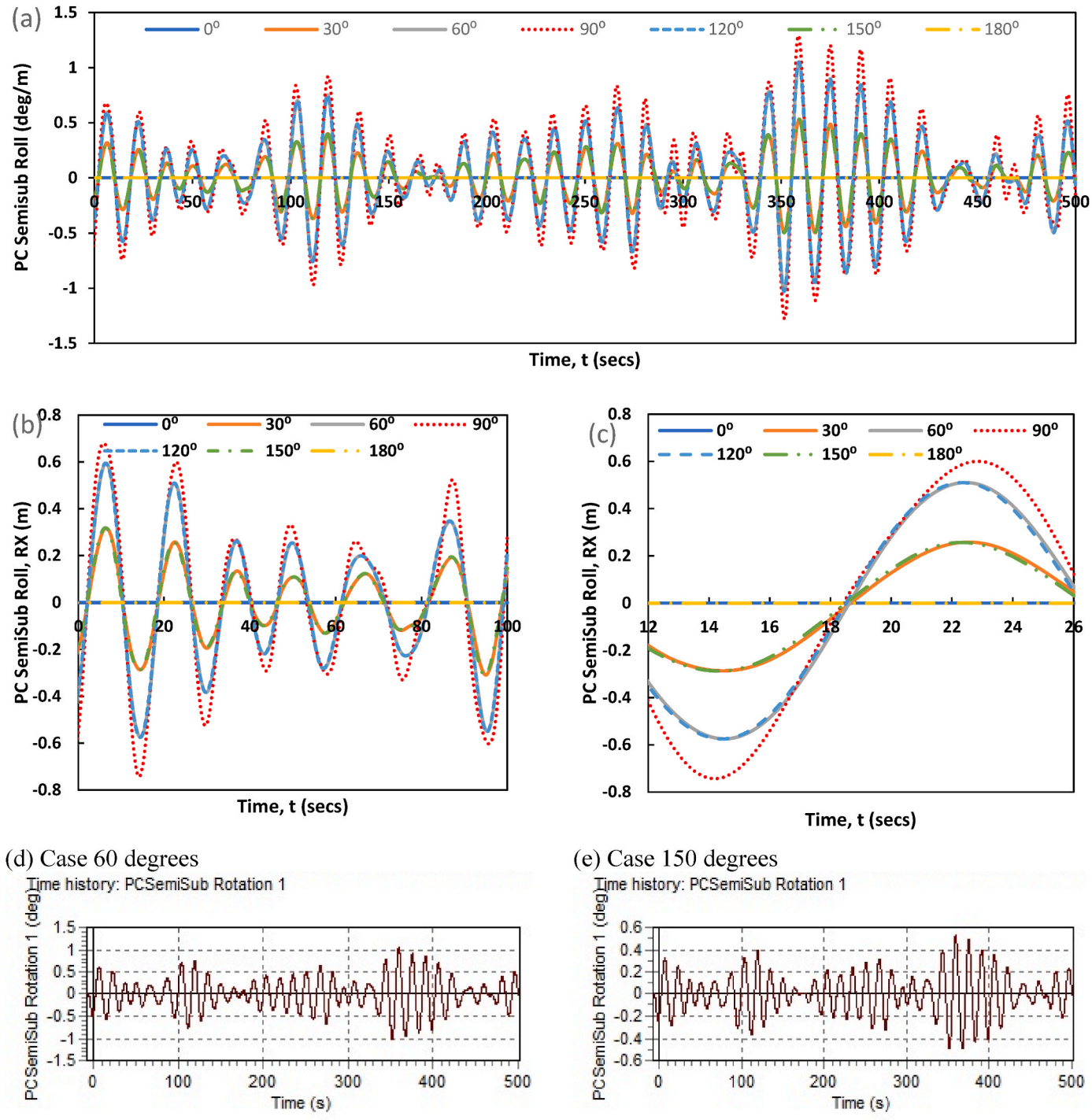

Fig. 28. Roll response of the Paired Column Semisubmersible.

conditions. On that note, the challenge of effectively analysing the mooring system for deep water application can be addressed. This study presented numerical investigations on mooring integration by considering different mooring configurations on the semisubmersibles. The research showed a detailed analysis based on the hydrodynamic studies on the mooring lines by considering damaged, intact, and all moorings. In addition, similar and dissimilar mooring cases were also investigated.

The model highlights of this paper are: firstly, the mooring designed for a Paired Column Semisubmersible (PCSemi) considered was the catenary mooring system. Secondly, there is a novelty in modelling the two configurations investigated: Chain-Polyester-Chain (CPC) and Polyester-Polyester (PP) configurations. Thirdly, there is a novelty in the modelling technique adopted for the mooring analysis, which is well presented. Fourthly, the tension and moment analysis of mooring lines attached to the fairleads of the PC-Semi are presented for different design configurations. Lastly, some novelty in the hydrodynamic loading effects on the paired-column semi-submersible conducted, for low frequency and wave frequency motions.

The study showed that the Chain-Polyester-Chain (CPC) configuration had higher tensions than the Polyester-Polyester (PP) configuration, which will be due to the stiffness of the materials. As such, the CPC configuration performed better and is more reliable for the PCSemi. This study gives the natural period of floating PCSemi's heave motion ranged from 21s to 22s. In addition, the CPC configuration has a smaller

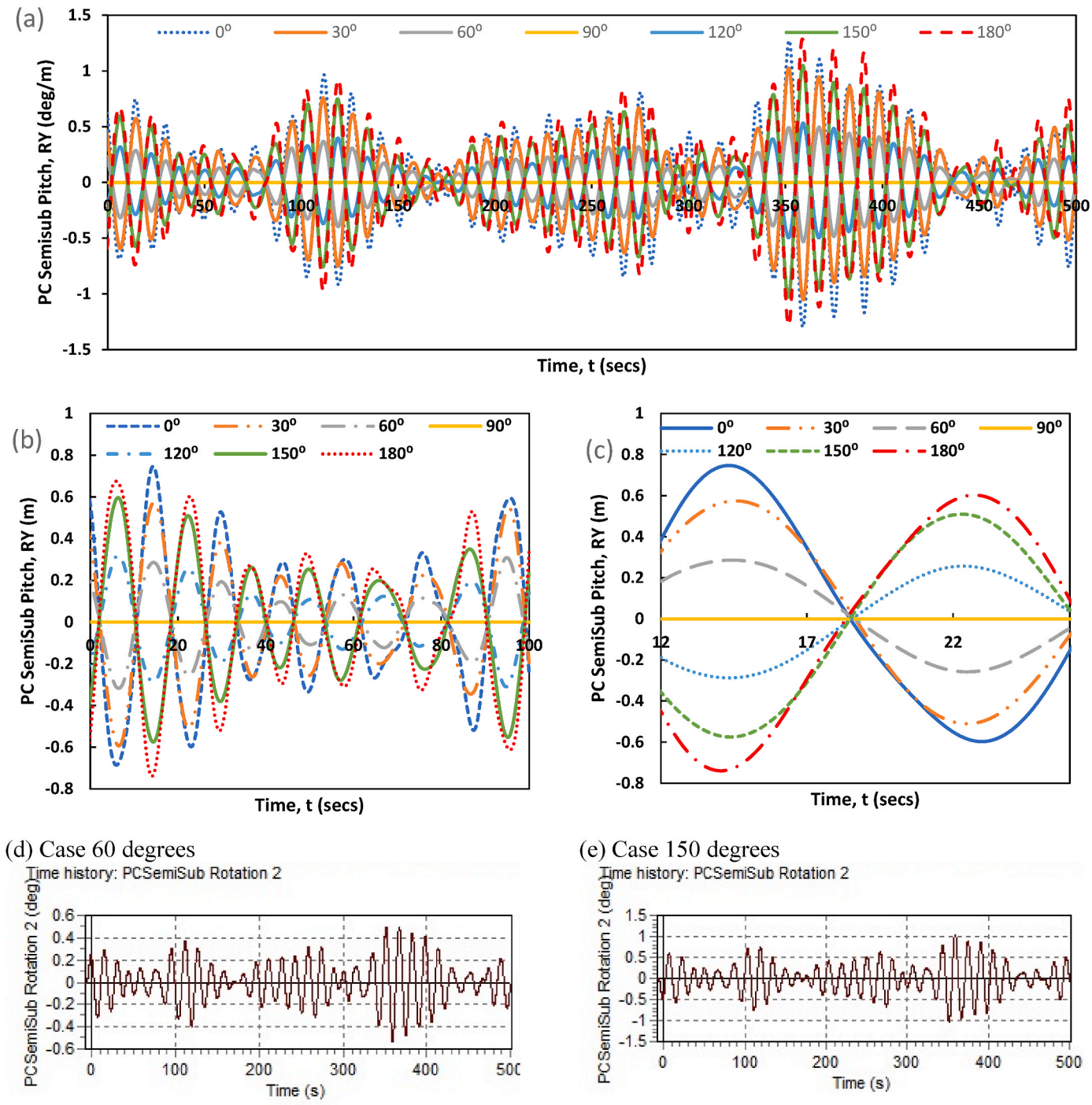

Fig. 29. Pitch response of the Paired Column Semisubmersible.

amplitude for wave-frequency platform motions in comparison to PP mooring configuration from the depicted PCSemi global performance. Also, the effect of a damaged mooring line increased the tension in other mooring lines. From this study, when one of the mooring lines is damaged, the response amplitude of the hull changes. This change might be small, but it depends on the type of mooring system considered. It will change since this is not a taut mooring system but a catenary mooring system, as depicted in Fig. 1. Thus, the reason for the offset seen in this Fig. 20, as the moorings help to offset some of the displacement in the model. Furthermore, the disparity observed between ML13 from other lines ML14, ML15 and ML16 occur when the model is not fully integrated, or has different bending and axial stiffnesses for the lines. Albeit, the catenary mooring system was adopted in the system, and the model was well validated. Recommendations made could be used during the review of existing industry mooring standards such as ISO (2013, 2019), API (1993), DNVGL (2015), OCIMF (1995, 2000), and ABS (2021a,b,c), where necessary. For instance, the choice of mooring line used when one of the mooring lines is damaged should be included in the standard or recommended guidance.

Data availability statement

The raw/processed data required to reproduce these findings cannot be shared at this time as the data also forms part of an ongoing study.

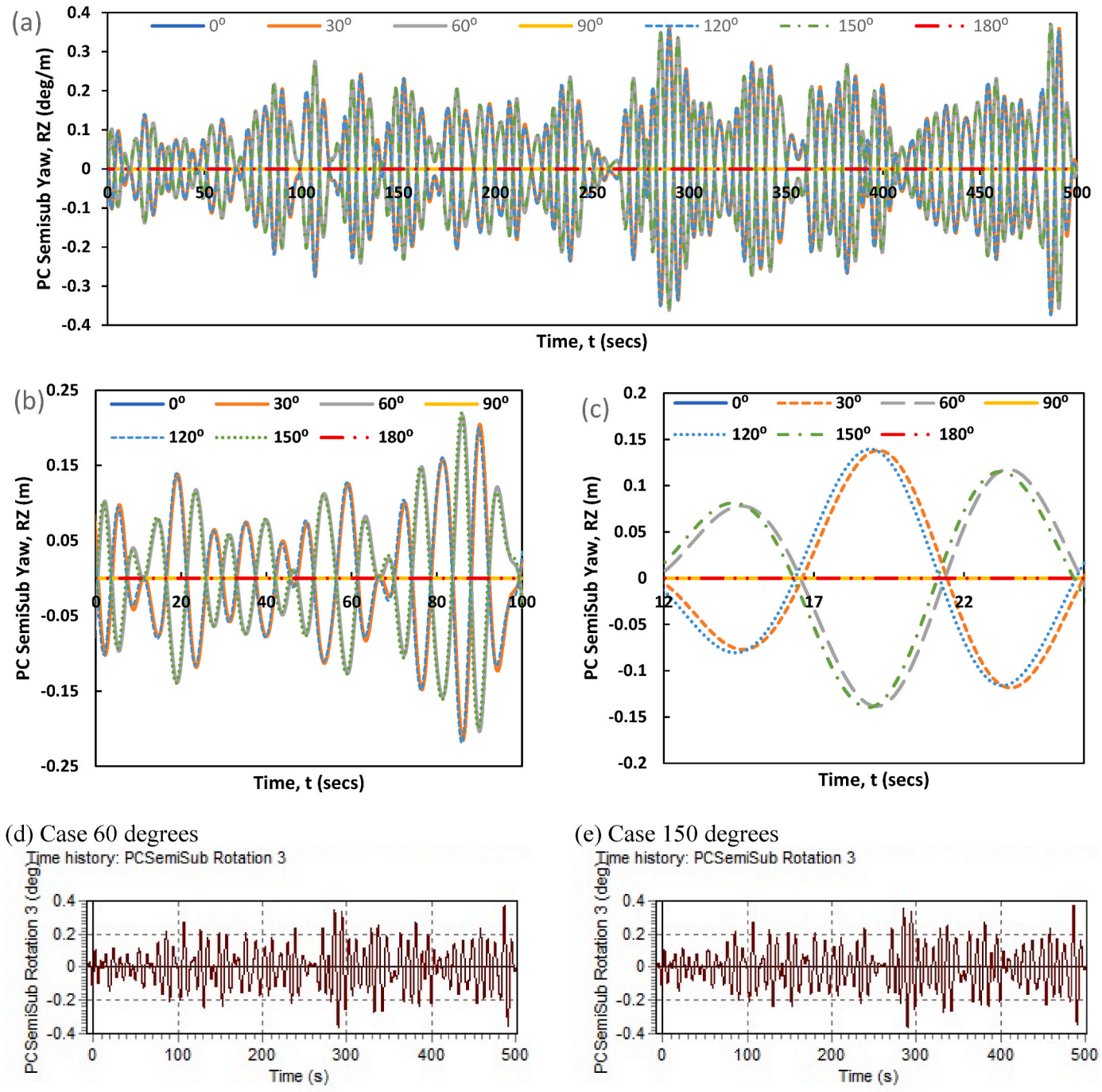

Fig. 30. Yaw response of the Paired Column Semisubmersible.

Funding

The funding support of Department of Engineering, Lancaster University, UK, and Engineering and Physical Sciences Research Council (EPSRC)'s DTC (Doctoral Training Centre), UK are highly appreciated on this project. In addition, the funding of Overseas Scholarships by the Niger Delta Development Commission (NDDC), Nigeria is much appreciated. The authors also acknowledge the support of Standards Organisation of Nigeria (SON), F.C.T Abuja, Nigeria. This mooring design is part of a research team for a PhD research and a BEng project in Lancaster University. Also, acknowledge National Natural Science Foundation of China (NSFC) for supporting the Project 51922064, including this study.

CRediT authorship contribution statement

Chiemela Victor Amaechi: Conceptualization, Methodology, Software, Validation, Formal analysis, Investigation, Resources, Data curation, Writing – original draft, Writing – review & editing, Visualization, Supervision, Funding acquisition, Project administration. **Agbomerie Charles Odijie:** Conceptualization, Methodology, Software, Validation, Formal analysis, Investigation, Resources, Data curation, Writing – review & editing, Visualization, Supervision, Project administration, Funding acquisition. **Facheng Wang:** Methodology, Validation, Formal analysis, Investigation, Writing – review & editing, Supervision, Funding acquisition. **Jianqiao Ye:** Conceptualization, Methodology, Software, Validation, Formal analysis, Investigation, Resources, Data

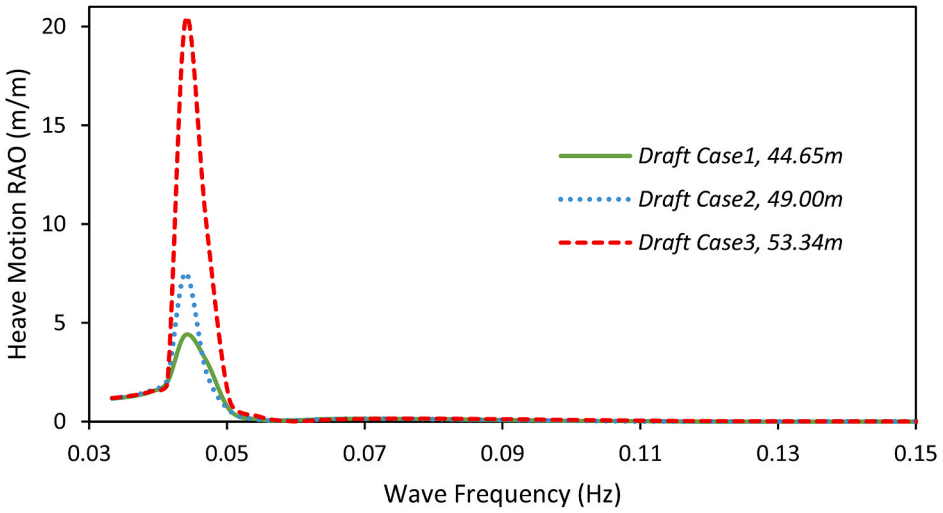

Fig. 31. Heave of Paired Column Semisubmersible at higher wave period, Tp of 17.2s.

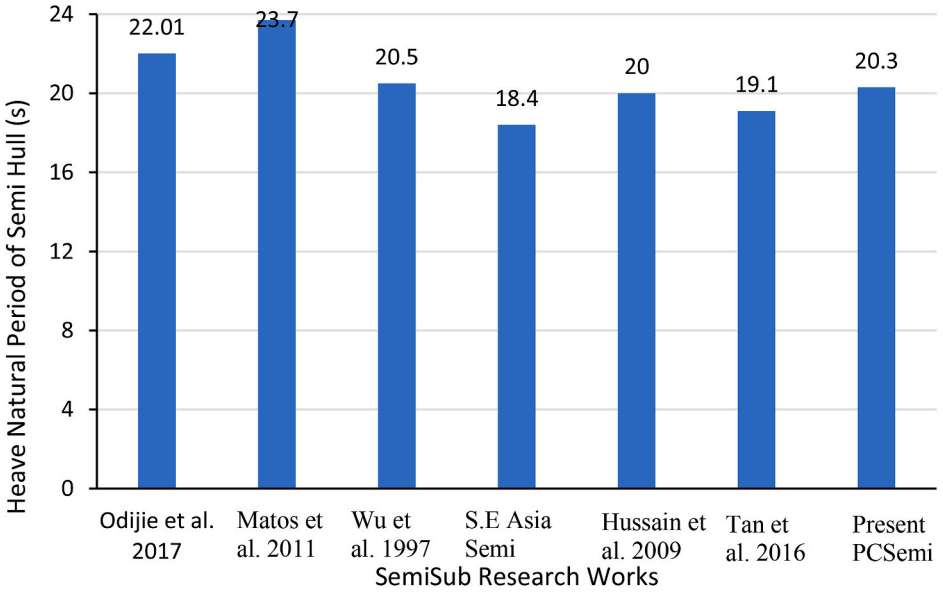

Fig. 32. Comparative semisubmersible hull profiles for Heave natural periods at max period of 17.2s.

curation, Writing – review & editing, Visualization, Supervision, Project administration, Funding acquisition.

Declaration of competing interest

The authors declare that they have no known competing financial interests or personal relationships that could have appeared to influence the work reported in this paper.

Acknowledgement

The authors acknowledge the technical support from Lancaster University Engineering Department staff – Andy Baker with necessary permissions to use Lab PCs during the COVID19 pandemic, and Andy Gavriluk for support with computational resources. The support from Mark Salisbury of Lancaster University for assistance with the fabrication of the Paired Column Semisubmersible Model for this research. The authors also acknowledge the earlier model ideas by Lancaster University research team, particularly Bhosale Darshan on the PCSemi mooring modelling. We also acknowledge Mohamed Milad of Lancaster University for his technical support during the Paired Column Semisubmersible experiment on the wave tank using the Imetrum system for DIC technique are all acknowledged. Also grateful to Abiodun K. Oyetunji of Lancaster University, Lancaster Environment Centre (LEC) for reviewing this manuscript. The authors also appreciate the reviewers for their comments.

References

Aboshio, A., Green, S., Ye, J., 2015. Experimental investigation of the mechanical properties of neoprene coated nylon woven reinforced composites. Compos. Struct. 120, 386–393. https://doi.org/10.1016/j.compstruct.2014.10.015. February 2015.

ABS (2021a). ABS FPI Guide- ABS Guide for Building and Classing Floating Production Installations, 2021. American Bureau of Shipping, USA. https://ww2.eagle.org/content/dam/eagle/rules-and-guides/current/offshore/82_rulebuildingandclassingfloatingproductioninstallations_2021/fpi-rules-jan21.pdf.

ABS (2021b). Rules for Building and Classing - Single Point Moorings, vol. 2014, no. July. Texas, USA: American Bureau of Shipping. Available at: https://ww2.eagle.org/content/dam/eagle/rules-and-guides/current/offshore/8_rules-forbuildingandclassingsinglepointmoorings_2021/spm-rules-jan21.pdf.

ABS (2021c). Guidance Notes on the Application of Synthetic Ropes for Offshore Mooring. American Bureau of Shipping, New York, USA. https://ww2.eagle.org/

content/dam/eagle/rules-and-guides/current/offshore/90_fiberrope_2021/fiber-rope-gn-june21.pdf.
Aggidis, G.A., Taylor, C.J., 2017. Overview of wave energy converter devices and the development of a new multi-axis laboratory prototype. IFAC-PapersOnLine 50 (1), 15651–15656. https://doi.org/10.1016/j.ifacol.2017.08.2391.
Aki, Taguchi, Takehito, Tomoi, 2001. A stamp of approval to mega-float airport feasibility: mega-float airport investigation committee within Ministry of Land, Infrastructure and transport of Japan has compiled their final report. Available at: http://www.mlit.go.jp/english/maritime/mega_float.html.
Ali, M.O.A., Ja'e, I.A., Zhen Hwa, M.G., 2020. Effects of water depth, mooring line diameter and hydrodynamic coefficients on the behaviour of deepwater FPSOs. Ain Shams Eng. J. 11 (3), 727–739. https://doi.org/10.1016/j.asej.2019.12.001.
Alonso, J. Juvinao Carbono, Menezes, Ivan F.M., Fernando Martha, Luiz, 2005. Mooring pattern optimization using genetic algorithms. In: 6th World Congresses of Structural and Multidisciplinary Optimization. Rio de Janeiro, 30 May - 03 June 2005, Brazil. Available at: https://web.tecgraf.puc-rio.br/~lfm/papers/CarbonoWCSMO2005.pdf.
Amaechi, C.V., Ye, J., 2017. A numerical modeling approach to composite risers for deep waters. In: International Conference on Composite Structures (ICCS20) Proceedings. France, Paris, 2017.
Amaechi, C.V., Ye, J., 2021. Local tailored design of deep water composite risers subjected to burst, collapse and tension loads. Ocean Eng. https://doi.org/10.1016/j.oceaneng.2021.110196, 2021.
Amaechi, C.V., Wang, F., Hou, X., Ye, J., 2019a. Strength of submarine hoses in Chinese-lantern configuration from hydrodynamic loads on CALM buoy. Ocean Eng. 171, 429–442. https://doi.org/10.1016/j.oceaneng.2018.11.010.
Amaechi, C.V., Ye, J., Hou, X., Wang, F.-C., 2019b. "Sensitivity studies on offshore submarine hoses on CALM buoy with comparisons for Chinese-lantern and lazy-S configuration OMAE2019-96755. In: 38th international conference on ocean, offshore and arctic engineering, Glasgow, Scotland, June 9–14, 2019, 2019.
Amaechi, C.V., Gillett, N., Odijie, A.C., Hou, X., Ye, J., 2019c. Composite risers for deep waters using a numerical modelling approach. Compos. Struct. 210 https://doi.org/10.1016/j.compstruct.2018.11.057.
Amaechi, C.V., Gillett, N., Odijie, A.C., Wang, F., Hou, X., Ye, J., 2019d. Local and global design of composite risers on Truss SPAR platform in deep waters, paper 20005. In: Proceedings of 5th International Conference on Mechanics of Composites, 2019, 20005, pp. 1–3.
Amaechi, C.V., Odijie, C., Sotayo, A., Wang, F., Hou, X., Ye, J., 2019e. Recycling of renewable composite materials in the offshore industry. In: Encyclopedia of Renewable and Sustainable Materials; Reference Module in Materials Science and Materials Engineering. https://doi.org/10.1016/B978-0-12-803581-8.11445-6.
Amaechi, C.V., Odijie, C., Etim, O., Ye, J., 2019f. Economic aspects of fiber reinforced polymer composite recycling. In: Encyclopedia of Renewable and Sustainable Materials; Reference Module in Materials Science and Materials Engineering. https://doi.org/10.1016/B978-0-12-803581-8.10738-6.
Amaechi, C.V.; Chesterton, C.; Butler, H.O.; Wang, F.; Ye, J. (2021a). Review on the design and mechanics of bonded marine hoses for Catenary Anchor Leg Mooring (CALM) buoys. Ocean. Eng. 2021; 242(7): 110062, 1-32, doi:.10.1016/j.oceaneng.2021.110062.
Amaechi, C.V., Wang, F., Ye, J., 2021b. Mathematical modelling of marine bonded hoses for single point mooring (SPM) systems, with catenary anchor leg mooring (CALM) buoy application—a review. J. Mar. Sci. Eng. 9 (11), 1–62. https://doi.org/10.3390/jmse9111179, 2021.
Amaechi, C.V., Chesterton, C., Butler, H.O., Wang, F., Ye, J., 2021c. An overview on bonded marine hoses for sustainable fluid transfer and (Un)Loading operations via floating offshore structures (FOS). J. Mar. Sci. Eng. 9 (11), 1236. https://doi.org/10.3390/jmse9111236, 2021.
Amaechi, C.V., Wang, F., Ye, J., 2021d. Understanding the fluid-structure interaction from wave diffraction forces on CALM buoys: numerical and analytical solutions. Ships Offshore Struct. 2021 https://doi.org/10.1080/17445302.2021.2005361.
Amaechi, C.V., Wang, F., Ye, J., 2021e. Numerical assessment on the dynamic behaviour of submarine hoses attached to CALM buoy configured as Lazy-S under water waves. J. Mar. Sci. Eng. 9 (1130), 1–48. https://doi.org/10.3390/jmse9101130, 2021.
Amaechi, C.V., Wang, F., Ye, J., 2021f. Numerical studies on CALM buoy motion responses and the effect of buoy geometry cum skirt dimensions with its hydrodynamic waves-current interactions. Ocean Eng. 2021. https://doi.org/10.1016/j.oceaneng.2021.110378.
Amaechi, C.V., Wang, F., Ye, J., 2022a. Investigation on hydrodynamic characteristics, wave–current interaction and sensitivity analysis of submarine hoses attached to a CALM buoy. J. Mar. Sci. Eng 10 (1), 120. https://doi.org/10.3390/jmse10010120, 2022.
Amaechi, C.V., Wang, F., Ye, J., 2022b. Experimental study on motion characterisation of CALM buoy hose system under water waves. J. Mar. Sci. Eng 10 (2), 204. https://doi.org/10.3390/jmse10020204, 2022.
Amaechi, C.V., Wang, F., Ja'e, I.A., Aboshio, A., Odijie, A.C., 2022c. A literature review on the technologies of bonded hoses for marine applications. Ships Offshore Struct. https://doi.org/10.1080/17445302.2022.2027682, 2022. (Accepted/In press).
Amaechi, C.V., Chesterton, C., Butler, H.O., Gu, Z., Odijie, A.C., Wang, F., Hou, X., Ye, J., 2022d. Finite element modelling on the mechanical behaviour of Marine Bonded Composite Hose (MBCH) under burst and collapse. J. Mar. Sci. Eng. (JMSE). https://doi.org/10.3390/jmse10020151.
Amaechi, C.V., Chesterton, C., Butler, H.O., Gu, Z., Odijie, A.C., Hou, X., 2022e. Numerical modelling on the local design of a Marine Bonded Composite Hose (MBCH) and its helix reinforcement. J. Compos. Sci. 6 (3), 79. https://doi.org/10.3390/jcs6030079, 2022.
Andrianov, A.O.I., 2005. Hydroelastic Analysis of very large floating structures. In: Doctoral Thesis in Delft University of Technology, p. 172. The Netherlands 2005. Available at: http://resolver.tudelft.nl/uuid:85cef785-c17c-41d7-9a58-6a183c468523.
ANSYS, 2017a. ANSYS Aqwa Theory Manual, Release, 18.2. ANSYS Inc, Canonsburg, USA.
ANSYS, 2017b. ANSYS Aqwa User's Manual, Release, 18.2. ANSYS Inc, Canonsburg, USA.
ANSYS, 2017c. ANSYS Meshing User's Guide, Release, 18.2. ANSYS Inc, Canonsburg, USA.
API (1993). API Recommended Practice (RP 2FP1), Analysis of Spread Mooring Systems for Floating Drilling Units, second ed., American Petroleum Institute, Texas, USA. Retrieved on: 7th May, 2021. Available at: https://pslcolombia.com/documentos/API%20RP%2002%20FP1%20Mooring%20FPS%201993.pdf.
API, 2007. API2Int-Met: Interim Guidance on Hurricane Conditions in the Gulf of Mexico. American Petroleum Institute, DC, USA. Available at. https://law.resource.org/pub/us/cfr/ibr/002/api.2int-met.2007.pdf.
Azcona, J., Munduate, X., González, L., Nygaard, T.A., 2017. Experimental validation of a dynamic mooring lines code with tension and motion measurements of a submerged chain. Ocean Eng. 129, 415–427. https://doi.org/10.1016/j.oceaneng.2016.10.051.
Bai, Y., Bai, Q., 2005. Subsea Pipelines and Risers. Elsevier Publishers.
Barltrop, N.D.P., 2003. Floating Structures: a Guide for Design and Analysis, one. Oilfield Publications Limited (OPL), Ledbury, England.
Bhosale, D., 2017. Mooring Analysis of Paired-Column Semisubmersible. BEng Dissertation, Engineering Department, Lancaster University.
Bishop, R.E.D., Price, W.G., 2005. Hydroelasticity of Ships. Cambridge University Press, Cambridge, UK. Revised Edition.
Brebbia, C.A., 1979. Dynamic Analysis of Offshore Structures. Newnes-Butterworths, London, UK.
Brorsen, M., 2006. Slowly-Varying 2nd Order Wave Forces on Large Structures. Aalborg University, Department of Civil Engineering.
Chen, X.H., 1997. Motion and mooring line loads of a moored semi-submersible in waves. In: Proceedings of the International Conference on Offshore Mechanics and Arctic Engineering– OMAE, pp. 235–241.
Daghigh, M., Paein Loulaei, R.T., Seif, M.S., 2002. Mooring system design and analysis for the flooding bridge of Urmia lake. In: 12th International Conference on Offshore Mechanics and Arctic Engineering. Oslo, Norway.
Das, S., Zou, J., 2015. Characteristic Responses of a Dry-Tree Paired-Column and Deep Draft Semisubmersible in Central Gulf of Mexico. 20th Offshore Symposium. Texas Section of the Society of Naval Architects and Marine Engineers At, Houston, TX.
Davies, P., Baron, P., Salomon, K., Bideaud, C., Labbe, J.P., Toumit, S., Francois, M., Grosjean, F., Bunsell, T., Moysan, A.G., 2008. Influence of fiber stiffness on deepwater mooring line response. In: 27th International Conference on Offshore Mechanics and Arctic Engineering, OMAE 2008-57147. Estoril, Portugal.
DNVGL, 2015. DNVGL-OS-E301: position mooring, offshore standard. Oslo, Norway: Det Norske Veritas & Germanischer Lloyd. Available at: https://rules.dnvgl.com/docs/pdf/dnvgl/os/2015-07/DNVGL-OS-E301.pdf.
Doyle, S., Aggidis, G.A., 2019. Development of multi-oscillating water columns as wave energy converters. In: Renewable and Sustainable Energy Reviews, vol. 107. Elsevier, pp. 75–86. https://doi.org/10.1016/j.rser.2019.02.021. C.
Doyle, S., Aggidis, G.A., 2021. Experimental investigation and performance comparison of a 1 single OWC, array and M-OWC. Renew. Energy 168. https://doi.org/10.1016/j.renene.2020.12.032. May 2021.
Falcão, A.F.O., 2010. Wave energy utilization: a review of the technologies. Renew. Sustain. Energy Rev. 14 (3), 899–918. https://doi.org/10.1016/j.rser.2009.11.003. April 2010.
Falcão, A.F.O., Henriques, J.C., 2016. Oscillating-water-column wave energy converters and air turbines: a review. Renew. Energy 85, 1391–1424. https://doi.org/10.1016/j.renene.2015.07.086. January 2016.
Garrett, D.L., 1982. Dynamic analysis of slender rods. ASME. J. Energy Resour. Technol. 104 (4), 302–306. https://doi.org/10.1115/1.3230419. December 1982.
Garrett, D.L., 2005. Coupled analysis of floating production systems. J. Ocean Eng. 32, 802–816.
Hasselmann, K., Barnett, T.P., Bouws, E., Carlson, H., Cartwright, D.E., Enke, K., Ewing, J.A., Gienapp, H., Hasselmann, D.E., Kruseman, P., et al., 1973. Measurements of wind-wave growth and swell decay during the Joint North Sea Wave Project (JONSWAP). In: In Ergänzungsheft zur Dtsch. Hydrogr. Z. -Hydraulic Engineering Reports; Ergänzungsheft 8-12; Reihe Vol. A80, Issue 12; 1973, 12. Deutches Hydrographisches Institut, Hamburg, Germany, pp. 1–90. Available online. http://resolver.tudelft.nl/uuid:f204e188-13b9-49d8-a6dc-4fb7c20562fc (accessed on 4 March 2022).
Heath, T.V., 2012. A review of oscillating water columns. Phil. Trans. R. Soc. A 370, 235–245. https://doi.org/10.1098/rsta.2011.0164.
Hirdaris, S.E., Bai, W., Dessic, D., Ergind, A., Gue, X., Hermundstad, O.A., Huijsmans, R., Iijima, K., Nielsen, U.D., Parunov, J., Fonseca, N., Papanikolaou, A., Argyriadis, K., Incecik, A., 2014. Loads for use in the design of ships and offshore structures. Ocean Eng. 78, 131–174. https://doi.org/10.1016/j.oceaneng.2013.09.012.
Huilong, R., Jian, Z., Guoqing, F., Hui, L., Chenfeng, L., 2009. Influence of Nonlinear Mooring Stiffness on Hydrodynamic Performance of Floating Bodies. OMAE 2009-79697.
Hussain, A., Nah, E., Fu, R., Gupta, A., 2009. Motion comparison between a conventional deep draft semi-submersible and a dry tree semi-submersible. In: Proceedings of the 28th International Conference on Ocean, Offshore and Arctic Engineering. Hawaii, USA, pp. 785–792. https://doi.org/10.1115/OMAE2009-80006.

Imetrum, 2016. Video Gauge User Manual: Version 5.4.0. Imetrum Limited, Bristol, UK, pp. 1–153.
Imetrum, 2017. Digital image correlation in Video Gauge. Available at: https://www.imetrum.com/documents/product-sheets/digital-image-correlation.pdf.
Irvine, H.M., 1981. Cable Structures. MIT Press, Cambridge, Massachusetts, USA.
ISO, 2013. ISO 19901-7:2013. Petroleum and Natural Gas Industries — Specific Requirements for Offshore Structures — Part 7: Stationkeeping Systems for Floating Offshore Structures and Mobile Offshore Units. International Organization for Standardization, Geneva, Switzerland.
ISO, 2019. ISO 9089:2019 Marine Structures — Mobile Offshore Units — Mooring Positioning Windlasses and Winches. International Organization for Standardization, Geneva, Switzerland.
Ja'e, I.A., Ali, M.O.A., Yenduri, A., Nizamani, Z., Nakayama, A., 2022. Optimisation of mooring line parameters for offshore floating structures: A review paper. Ocean Eng. 247, 110644. https://doi.org/10.1016/j.oceaneng.2022.110644, 1 March 2022.
Jordan, M.A., Beltran-Aguedo, R., 2004. Nonlinear identification of mooring lines in dynamic operation of floating structures. J. Ocean Eng. 31, 455–482.
Kim, C.H., 2008. Nonlinear Waves and Offshore Structures. World Scientific, Hackensack, New Jersey, USA.
Kim, S.J., Spernjak, D., Mejia-Alvarez, R., Vinayan, V., Sterenborg, J., Antony, A., Holmes, S., Halkyard, J., 2018. Numerical simulation of vortex-induced motion of a deep-draft paired-column semi-submersible offshore platform. Ocean Eng. 149, 291–304. https://doi.org/10.1016/j.oceaneng.2017.12.019.
Langley, R.S., 1984. The statistics of second order wave forces. Appl. Ocean Res. 6 (4), 182–186.
Lassen, T., Storvoll, E., Bech, A., 2009. Fatigue life prediction drilling ship of mooring chains subjected to tension and out of plane bending. In: 28th International Conference on Offshore Mechanics and Arctic Engineering, OMAE 2009-79253, Honolulu, Hawaii, USA.
Loukogeorgaki, E., Angelides, D., 2005. Stiffness of mooring lines and performance of floating breakwater in three dimensions. Appl. Ocean Res. 27 (4), 187–208. https://doi.org/10.1016/j.apor.2005.12.002.
Ma, G., Sun, L., Wang, H., 2009. The analysis of mooring systems of a drillship. In: 28th International Conference on Offshore Mechanics and Arctic Engineering, OMAE 2009- 79320, Honolulu, Hawaii, USA.
Maffra S., Pacheo C. & Menezez M., 2003, "Genetic algorithm optimization for mooring system", Rio de Janeiro, Brazil. Available at: https://citeseerx.ist.psu.edu/viewdoc/download?doi=10.1.1.115.7297&rep=rep1&type=pdf.
Mazaheri, S., Incesik, A., 2004. Predicting the maximum mooring force of a moored floating offshore structure. In: 23rd International Conference on Offshore Mechanics and Arctic Engineering OMAE 2004-51245. British Columbia, Vancouver. Canada.
Mazaheri, S., Mesbahi, E., 2003. Sea keeping analysis of a Turret-moored FPSO by using artificial neural networks. OMAE 2003-37148. In: 22nd International Conference on Offshore Mechanics and Arctic Engineering. Cuncun, Mexico.
Milad, M., Green, S., Ye, J., 2018. Mechanical properties of reinforced composite materials under uniaxial and planar tension loading regimes measured using a non-contact optical method. Compos. Struct. 202, 1145–1154. https://doi.org/10.1016/j.compstruct.2018.05.070.
Mirzaei, Mahdi, et al., 2014. Mooring pattern optimization using A genetic algorithm. Jurnal Teknologi (Sci. Eng.) 66 (2), 189–193. Available at: https://core.ac.uk/download/pdf/42921471.pdf.
Morch, M., Moan, T., 1985. Comparison between measured and calculated behavior of a moored semi-submersible platform. Dev. Mar. Technol. 2, 175–186.
Morison, J.R., Johnson, J.W., Schaaf, S.A., 1950. The force exerted by surface waves on piles. J. Pet. Technol 2 (1950), 149–154. https://doi.org/10.2118/950149-G.
Matos, V.L.F., Simos, A.N., Sphaier, S.H., 2011. Second-order resonant heave, roll and pitch motions of a deep-draft semi-submersible: Theoretical and experimental results. Ocean Eng. 38 (17–18), 2227–2243. https://doi.org/10.1016/j.oceaneng.2011.10.005.
Newman, J.N., 1974. Interaction of water waves with two closely spaced vertical obstacles. J. Fluid Mech. 66 (1), 97–106. https://doi.org/10.1017/S0022112074000085.
Newman, J.N., 1999. Radiation and diffraction analysis of the McIver toroid. J. Eng. Math. 35 (1–2), 135–147. https://doi.org/10.1023/A:1004391615875.
OCIMF, 1995. Single Point Mooring Maintenance and Operations Guide (SMOG). Witherby & Co. Ltd, London, UK, 1995.
OCIMF, 2000. OCIMF: Guidelines for the Purchasing, Prototype Testing and Production of SPM Hawsers, 2000. Oil Companies International Marine Forum, London.
Odijie, A.C., 2016. In: Design of Paired Column Semisubmersible Hull. PhD Thesis Lancaster University, Engineering Department, Lancaster, UK. https://doi.org/10.17635/lancaster/thesis/39. Available at:
Odijie, C., Ye, J., 2015a. Effect of vortex induced vibration on a paired column semi-submersible platform. Int. J. Struct. Stabil. Dynam. 15 (8), 1540019. https://doi.org/10.1142/S0219455415400192, 2015.
Odijie, C., Ye, J., 2015b. Understanding fluid-structure interaction for high amplitude wave loadings on a deep-draft paired column semi-submersible platform:A finite element approach. In: Presented at the International Conference on Light Weight Design of Marine Structures. Glasgow, United Kingdom, 2015.
Odijie, A.C., Quayle, S., Ye, J., 2017a. Wave induced stress profile on a paired column semisubmersible hull formation for column reinforcement. Eng. Struct. 143, 77–90. https://doi.org/10.1016/j.engstruct.2017.04.013. Available at:
Odijie, A.C., Wang, F., Ye, J., 2017b. A review of floating semisubmersible hull systems: column stabilized unit. Ocean. Eng. 144, 191–202. https://doi.org/10.1016/j.oceaneng.2017.08.020. Available at:
Okamura, Hideo, 2000. Realizing the world's first floating airport. JSCE J. http://www.jsce.or.jp/kokusai/civil_engineering/2000/realizing.pdf.
Orcina, 2014. OrcaFlex Manual, Version 9.8a, Ulverton, Cumbria, UK: Orcina Ltd. Available at: https://www.orcina.com/SoftwareProducts/OrcaFlex/Documentation/index.php ..
Orcina (2021a). Orcaflex line model. Available at: https://www.orcina.com/webhelp/OrcaFlex/Content/html/Linetheory,Structuralmodeldetails.htm Accessed 13 April 2021..
Orcina, 2021b. Orcaflex theory: overview. Available at: https://www.orcina.com/webhelp/OrcaFlex/Content/html/Linetheory,Overview.htm.
Pierson, W.J., Moskowitz, L., 1964. A proposed spectral form for fully developed wind seas based on the similarity theory of SA Kitaigorodskii. J. Geophys. Res. Space Phys. 69, 5181–5190. https://doi.org/10.1029/JZ069i024p05181.
Pimenta, F., Ruzzo, C., Failla, G., Arena, F., Alves, M., Magalhães, F., 2020. Dynamic response characterization of floating structures based on numerical simulations. Energies 13, 5670. https://doi.org/10.3390/en13215670, 2020.
Rezvani, A., Shafieefar, M., 2007. Mooring optimization of floating platforms using a genetic algorithm. Ocean Eng. 34, 1413–1421.
RPSEA, 2009. Ultra Deepwater Dry Tree System for Drilling and Production. Research Partnership to Secure Energy for America.
RPSEA (2014a). Ultra-deepwater dry tree system for drilling and production in the Gulf of Mexico. Dry tree semi conceptual design report. Research Partnership to Secure Energy for America. RPSEA Project Number 10121-4405-02. Pages 1-101 https://rpsea.org/sites/default/files/2018-06/10121-4405-02-FR-UDW_Dry_Tree_System_Drilling_Production_GOM_Appendix_A2-12-30-14_P.pdf.
RPSEA (2014b). Ultra-Deepwater Dry Tree System for Drilling and Production in the Gulf of Mexico, Phase 2. Conceptual Design Report, RPSEA & Houston Offshore. H12122-G-RPT-GN-15001 https://rpsea.org/sites/default/files/2018-06/10121-4405-02-FR-UDW_Dry_Tree_System_Drilling_Production_GOM_Appendix_A1-12-30-14_P.pdf.
Sabziyan, Hadi, Hassan, Ghassemi, Azarsina, Farhood, Kazemi, Saeid, 2014. Effect of mooring lines pattern in a semi-submersible platform at surge and sway movements. J. Ocean Res. 2 (No. 1), 17–22. https://doi.org/10.12691/jor-2-1-4, 2014.
Sarpkaya, T.S., 2010. Wave Forces on Offshore Structures. Cambridge University Press, Cambridge, London, UK.
Servan-Camas, B., Gutierrez-Romero, J.E., Garcia-Espinosa, J., 2018. A time-domain second-order FEM model for the wave diffraction-radiation problem. Validation with a semisubmersible platform. Mar. Struct. 58, 278–300. https://doi.org/10.1016/j.marstruc.2017.12.001. March 2018.
Ohmatsu, Shigeo, 2005. Overview: research on wave loading and responses of VLFS. Mar. Struct. 18 (2), 149–168. https://doi.org/10.1016/j.marstruc.2005.07.004.
Stansberg, C.T., 2008. Current effects on a moored floating platform in a Sea state. In: 27th International Conference on Offshore Mechanics and Arctic Engineering. OMAE, Estoril, Portugal, p. 57621, 2008.
Su-xia, Z., You-gang, T., Hai-xiao, L., 2009. Study on snap tension in mooring lines of deepwater platform. In: 28th International Conference on Offshore Mechanics and Arctic Engineering. OMAE, Honolulu, Hawaii, USA, p. 79881, 2009.
Suzuki, H., 2005. Overview of mega-float: concept, design criteria and analysis and design. Mar. Struct. 18 (2), 111–132. https://doi.org/10.1016/j.marstruc.2005.07.006.
Tan, J.H., Kiprawi, F., Kyoung, J., Sullivan, J.F.O., Nazri, J.A., 2016. Dry tree semisubmersible for cost-effective deepwater development. In: Proceedings of the Offshore Technology Conference Asia, Kuala Lumpur, Malaysia, March 22-25, 2016. https://doi.org/10.4043/26641-MS.
Waals, O.J., 2009. The effect of wave directionality on low frequency motions and mooring forces. In: 28th International Conference on Offshore Mechanics and Arctic Engineering. OMAE, Honolulu, Hawaii, USA, p. 79412, 2009.
Wang, C.M., Watanabe, E., Utsunomiya, T., 2008. Very Large Floating Structures, first ed. Routledge, Taylor & Francis Group, SPON Research, CRC Press, New York, USA.
Wang, Y., Xu, S., Wang, L., Wang, X., 2018. Motion responses of a catenary-taut-tendon hybrid moored single module of a semisubmersible-type VLFS over uneven seabed. J. Mar. Sci. Technol. https://doi.org/10.1007/s00773-018-0587-6.
Weller, S., Davies, P., Johanning, L., Banfield, S., 2013. Guidance on the use of synthetic fibre ropes for marine energy devices. A report prepared as part of the MERiFIC Project. In: Marine Energy in Far Peripheral and Island Communities". Ifremer Report Reference: RDT CSM 13-232. MERiFIC & ERDF, France. Available at: https://core.ac.uk/download/pdf/77031428.pdf.
Wichers, J., 2013. Guide to Single Point Moorings. VMooring & CreateSpace Independent Publishing.
Wilson James, F., 2008. Dynamics of Offshore Structures, second ed. Wiley Publishers.
Wu, S., 1997. The motions and internal forces of a moored semisubmersible in regular waves. Ocean Eng. 24 (7), 593–603.
Yamaguchi, H., Endo, K., Yamaguchi, H., 2005. Wave drift forces and moments on two ships arranged side by side in waves. Ocean Eng.
Ye, J., Cai, H., Liu, L., Zhai, Z., Amaechi, C.V., Wang, Y., Wan, L., Yang, D., Chen, X., Ye, J., 2020. Microscale intrinsic properties of hybrid unidirectional/woven composite laminates: Part I: experimental tests. Compos. Struct. 262, 113369. https://doi.org/10.1016/j.compstruct.2020.113369.
Zou, J., 2008. Dynamic responses of a dry tree semisubmersible platform with Ram style tensioners in the post-katrina irregular seas. In: International Society of Offshore and Polar Engineering Conference, 2008, Vancouver, Canada.
Zou, J., 2012. Semisubmersible platforms with steel catenary risers for western Australia and Gulf of Mexico. Ocean Syst. Eng. 2 (2), 99–113. https://doi.org/10.12989/ose.2012.2.2.099.
Zou, J. (2014). VIM response of a dry tree paired-column semisubmersibles platform and its effects on mooring fatigue. Society of naval architects and marine engineers. Paper Presented at the SNAME 19th Offshore Symposium, Houston, Texas, February

6, 2014. Available at: https://onepetro.org/SNAMETOS/proceedings-abstract/TOS14/1-TOS14/D013S006R002/3701 (Accessed on: 4 December, 2021).

Zou, J., 2017. Conceptual study of A paired-column semi-submersible platform for a 1.5 MTPA FLNG. In: Proceedings of the 22nd Offshore Symposium. SNAME 2017, Houston, Texas, pp. 1–39.

Zou, J., Chianis, J., 2011. Paired-column semisubmersible platform for wet tree with steel catenary riser application in offshore western Australia. In: 1st International Conference on Ocean System Engineering, ASEM'11PLUS: the 2011 World Congress on Advances in Structural Engineering and Mechanics. Seoul, Korea.

Zou J., Harrell R. (2017). New semisubmersible design increases safety, lower costs, improves project delivery time and is riser friendly. White paper, Houston offshore new semi design, USA. Available At: https://www.researchgate.net/publication/330259811_Houston_Offshore_New_Semi_Design (Accessed on: 4 December, 2021).

Zou, J., Poll, P., Roddier, D., Tom, N. & Peiffer, A. (2013). Vim testing of a paired column semi-submersible. Proceedings of International Conference on Ocean, Offshore and Arctic Engineering, June 9-14, 2013, Nantes, France. OMAE2013-10001. Volume vol. 7: CFD and VIV. DOI: 10.1115/OMAE2013-10001.

Zou, J., Poll, P., Antony, A., Das, S., Padmanabhan, R., Vinayan, V. & Parambath, A. (2014a). VIM model testing and VIM induced mooring fatigue of a dry tree paired column semisubmersible platform. Paper Number: OTC-25427-MS. Paper Presented at the Offshore Technology Conference, Houston, Texas, May 5-8, 2014. https://doi.org/10.4043/25427-MS.

Zou, J., Poll, P., Antony, A., Das, S., Padmanabhan, R., Vinayan, V., Parambath, A., 2014b. VIM model testing and VIM induced mooring fatigue of a dry tree paired-column semisubmersible platform. In: Offshore Technology Conference. https://doi.org/10.4043/25427-ms.